

A PALEOMAGNETIC STUDY
OF THE COASTAL PLUTONIC
COMPLEX OF NORTHERN CHILE

By LISA CHISHOLM

A thesis submitted to the
Graduated School-New Brunswick
Rutgers, The State University of New Jersey
in partial fulfillment of the requirements
for the degree of
Master of Science
Graduate Program in Geological Sciences

Written under the direction of
Professor Randall D. Forsythe
and approved by

Michael J. Carr

Ryan H. King

New Brunswick, New Jersey

January 1990

ABSTRACT OF THE THESIS

A Paleomagnetic Study of the Coastal Plutonic Complex of Northern Chile

by LISA CHISHOLM

Paleomagnetic results from seventy-six samples of six sites in the Jurassic to Cretaceous plutons of the Coastal Cordillera of northern Chile yielded stable remanent magnetization directions. These plutons have radiometric ages of from 157 to 128 Ma.. The plutons record both a normal, and a reversed, characteristic direction. The mean normal direction has a declination of 3.4° , an inclination of -38.5° , and an α_{95} of 10.5° . The mean reversed direction has a declination of 207.8° , an inclination of 33.8° , and an α_{95} of 10.8° . Paleopoles calculated from these mean directions have the positions of latitude= 85.8°N , longitude= 338.2°E and latitude= 63.5°S , longitude= 191.9°E respectively. In comparison to an APW path, the reversed pole indicates a clockwise rotation of approximately 28° , similar to other regional results. The normal pole is concordant with the present day magnetic field with no evidence for recent tectonic rotation. In a discussion of the relevance of this data to existing models for block rotation in the Andes, it is suggested that the mechanical consequences brought about by the migration of magmatism has been an important controlling factor. Magmatism is hypothetically viewed as a sensitizing agent within the mountain belt for deformation related to oblique subduction.

ACKNOWLEDGEMENT AND DEDICATION

This thesis would not have been completed without Sergio, who kept the old white 1972 pickup truck in running order even under extraordinary conditions. With the help of string and tape, Randy kept the drill alive until after my samples were drilled. This project also owes alot to friends, like Elena, who listened to me when I moaned and groaned about graduated school and to friends, like Beth, Craig, and Ken, with whom I shared many moments of total silliness.

This is dedicated to my advisor, Randy Forsythe, who gave me large doses of encouragement when I was ready to quit, and to the secretaries of the Department of Geological Sciences, Dee Daley and Carol Hammond, who gave me constant help and support.

TABLE OF CONTENTS

Abstract.....	ii.
Acknowledgment and Dedication.....	iii.
List of Tables.....	vi.
List of Illustrations.....	vii.
Introduction.....	1.
Geologic Background.....	4.
Paleomagnetic Technique.....	15.
<i>Component Analysis</i>	19.
Paleomagnetic Results.....	21.
<i>Site JBEA</i>	24.
<i>Site JSBE</i>	27.
<i>Site JPPA</i>	29.
<i>Site JPMA</i>	31.
<i>Site JPCA</i>	33.
<i>Site KQDA-D</i>	36.
<i>Lightning Strikes</i>	38.
<i>Viscous Samples</i>	46.
<i>Unreadable Labels</i>	46.
Discussion	
<i>Summary of Results</i>	50.
<i>The APW for South America</i>	53.
<i>Other Regional Results</i>	56.
<i>Andean Paleomagnetic Data</i>	61.
<i>Models</i>	64.
<i>Oroclinal bending</i>	64.
<i>Oblique Subduction Models</i>	64.

<i>An 'Indenter' analog.....</i>	66.
<i>Summary of models.....</i>	67.
References.....	69.

LIST OF TABLES

Table 1. - Paleomagnetic results from the Coastal Plutonic Complex.....	page 25.
Table 2. - Published paleomagnetic results from the Western Andes of Peru and Chile	page 58.

LIST OF ILLUSTRATIONS

Figure 1. -	Location map of the study area	page 2.
Figure 2. -	Geologic map with site locations.....	page 5.
Figure 3. -	Jurassic-Early Cretaceous arc and back-arc basins of the Central and Southern Andes.....	page 7.
Figure 4. -	Cross-section of the Jurassic-Early Cretaceous arc and back-arc basin of northern Chile.....	page 8.
Figure 5. -	Cross-section of Northern Chile in the Middle Cretaceous.....	page 10.
Figure 6. -	Map view of the axes of magmatism in northern Chile from the Jurassic to the present.....	page 12.
Figure 7. -	Major fault zones along the coast of Chile.....	page 13.
Figure 8. -	Bar graph of the coercivity range of the magnetic components used to calculate the site mean directions for this study.....	page 22.
Figure 9. -	The coercivity spectra of the magnetic components used to calculate the site mean directions for this study.....	page 23.
Figure 10.-	Typical Zijdeveld and J/J_0 plots for site JBEA.....	page 26.
Figure 11. -	Typical Zijdeveld and J/J_0 plots for site JSBE.....	page 28.
Figure 12. -	Typical Zijdeveld and J/J_0 plots for site JPPA.....	page 30.
Figure 13. -	Zijdeveld and J/J_0 plots of JPPA-3 after undergoing additional thermal demagnetization.....	page 32.
Figure 14. -	Typical Zijdeveld and J/J_0 plots for site JPMA.....	page 34.
Figure 15. -	Typical Zijdeveld and J/J_0 plots for site JPCA.....	page 35.

Figure 16. - Zijerveld and J/J_0 plots of samples JPCA-1,2,4-under AF and thermal demagnetization.....	page 37.
Figure 17. - Typical Zijderveld and J/J_0 plots for site KQDA-D.....	page 39.
Figure 18. - Zijderveld plots of suspected lightning strikes from site KSVM.....	page 41.
Figure 19. - J/J_0 plot of suspected lighting strikes from site KSVM.....	page 42.
Figure 20. - Zijderveld plots of suspected lightning strikes from site KCCA.....	page 44.
Figure 21. - J/J_0 plot of suspected lighting strikes from site KCCA.....	page 45.
Figure 22. - Typical Zijderveld and J/J_0 plots for site JCBA.....	page 47.
Figure 23. - Zijderveld and J/J_0 plots for site KQPA.....	page 48.
Figure 24. - Map showing site mean declinations and their alpha 95 values	page 51.
Figure 25. - Polar projection map showing an averaged APW path together with the normal and reversed poles calculated for the plutons of this study.....	page 52.
Figure 26. - Predicted versus observed declinations and inclinations for six sites of this study.....	page 54.
Figure 27. - Predicted versus observed declination and inclinations for the mean normal and reversed results.....	page 57.
Figure 28. - Predicted versus observed declination and inclinations for calculated mean components from the regional data.....	page 60.
Figure 29.- Published paleomagnetic poles from the western Andean ranges plotted on a polar projection map together with an averaged APW path.....	page 62.

INTRODUCTION

This study focuses on a paleomagnetic investigation of Jurassic to Cretaceous plutons exposed in the Coastal Ranges of Northern Chile between latitudes of 24° to 25°S (fig.1). This is the fourth comprehensive paleomagnetic study done in the Coastal Ranges of the Atacama Desert. It is the first to concentrate on the plutonic units of the area. These plutonic units, together with a coeval volcanic series originally referred to as the La Negra Formation (Garcia, 1967), are believed to represent a calc-alkaline arc that developed along the western margin of southern South America immediately west of a major marine back arc basin ('Andean Geosyncline') (Mpodozis and Ramos, in prep.). Today, the coastal plutonic units have been uplifted and separated from equivalent units to the west by the Atacama Fault Zone which has been suggested to have been the loci of strike-slip movement in Early Cretaceous (Arabaz, 1971).

The goal of this paleomagnetic study was to further the understanding of the tectonic development of the Coastal Cordillera. In recent years, a number of other paleomagnetic studies have revealed a complex pattern of rotations within the coastal province of Peru and Chile. This has created a framework in which the present study's results can be examined.

In the text to follow, there will first be a brief discussion of the geology of the sampling area. This will be

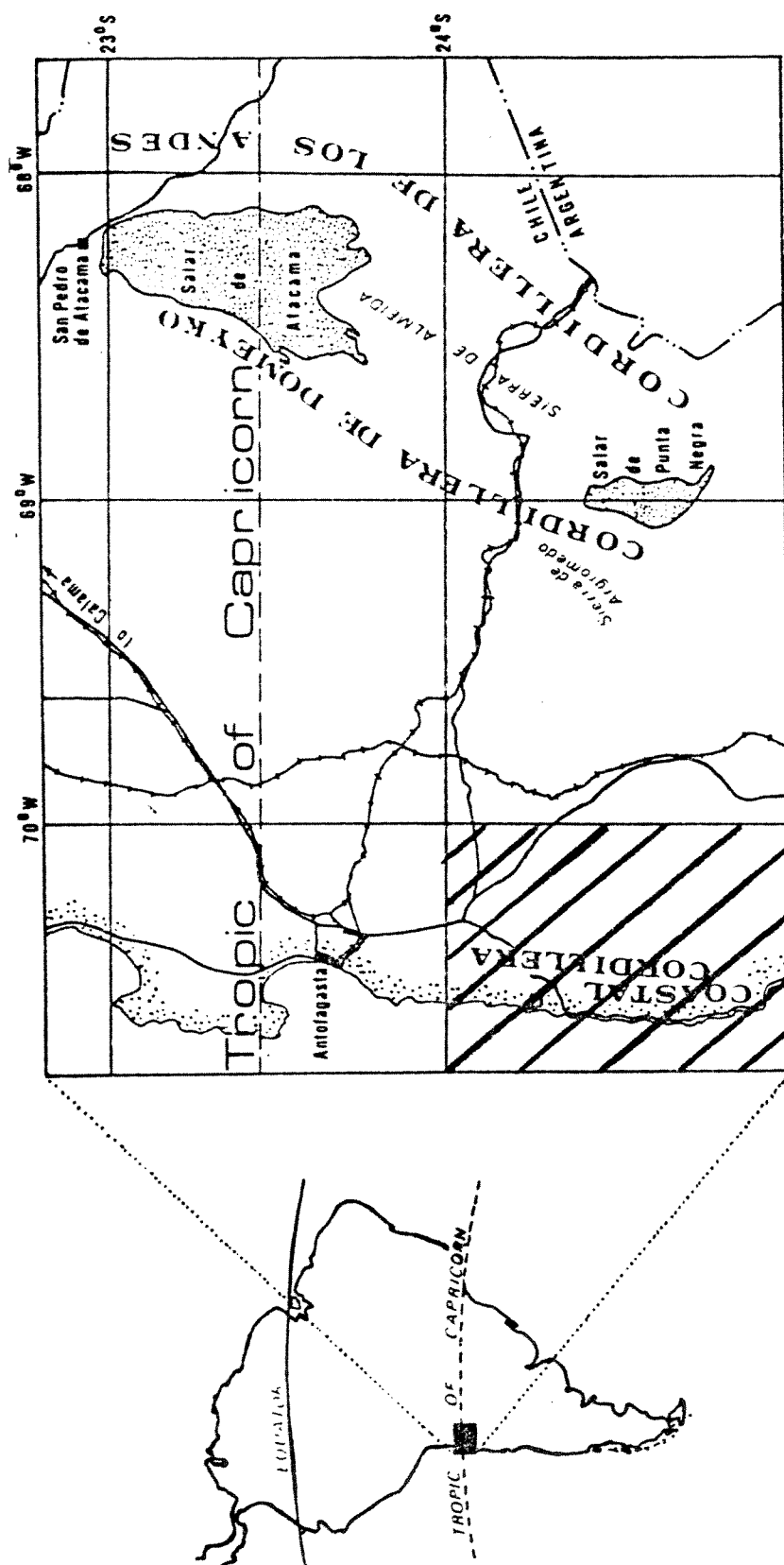


Figure 1. Location map of South America, hatched section shows general collecting location

followed by a discussion of paleomagnetic techniques. The laboratory results will be presented in detail. Then these results will be compared with other South American paleomagnetic data. Finally, observations from this pool of data and the comparisons will be used to test various tectonic models for Mesozoic and Cenozoic development of the Andes.

GEOLOGIC BACKGROUND

The geology of the sample area is shown in a simplified manner in figure two. The oldest unit, 'Paleozoic Basement', is a generic name for a collection of plutonic and metamorphic rocks that represent various morphologic elements of the region's Gondwana-history (see Dalziel and Forsythe, 1982; Coira et al, 1982; Bahlburg et al., 1987). The 'Mesozoic Coastal Batholith' is composed of gabbros, granodiorites, granites, late stage aplites, and various mafic to intermediate dike swarms that in the sampling area range in age from 128 to 157 Ma. (see Table 1). The Coloso Fm. (Late Cretaceous red beds) of Turner et al, 1984, the La Negra Fm. (Jurassic volcanics), and the El Way Formation (Hauterivian marine carbonates) of Hartley et al, 1988 are included under the label of 'Mesozoic Volcanics and Sedimentary Rocks'. Under the label of 'Cenozoic Rocks and Unconsolidated Cover' are included the Tertiary and Quaternary aeolian and shallow marine sandstones and gravels that unconformably overlie the older units (Ferraris and DiBiase, 1978) along the coastal margin. Structurally the region is broken up by high angle faults. While exposures of the faults are rare, most are inferred to be high angle (Ferraris and DiBiase, 1978). The bulk of these trend subparallel to the coast and are part of the Atacama Fault Zone (discussed below).

The plutonic basement and metasedimentary units of

Paleozoic age are thought by some to represent the evolution of a parautochthonous Arequipa microplate (Forsythe et al., in prep.). Paleomagnetic evidence (Forsythe, et al; 1988) demonstrates that this microplate probably collided with cratonic South America, then a part of Gondwana, prior to the Middle Devonian. Furthermore, paleomagnetic studies by Jesinkey, et al. (1987) have documented Late Carboniferous magnetizations that are concordant with the cratonic South American (Gondwana) apparent polar wander (APW) path. The units sampled by Jesinkey and others are exposed in the higher elevations of the Atacama Desert, approximately 80 km. to the east and southeast of those sampled here. Although these results were derived from units exposed to the east of the Coastal Ranges, there is some isotopic and lithostratigraphic similarity that argues for the Paleozoic basement of the Coastal Ranges being an integral part of the Arequipa microplate.

In the beginning of the Mesozoic, a magmatic arc and an associated ensialic back arc basin were developed within the Late Paleozoic basement (fig. 3). The marine basin expanded northward during the Early Jurassic in a back arc extensional regime and was filled with shallow water marine carbonate and terrigenous sediments. At the same time, intensive volcanism and plutonism built a linear magmatic arc called the La Negra Arc along the Coastal Range (fig. 4). The radiometric ages of resulting rocks of this event range from 190 to 115 Ma. (Maksaev, 1984; Boric et al, 1985).

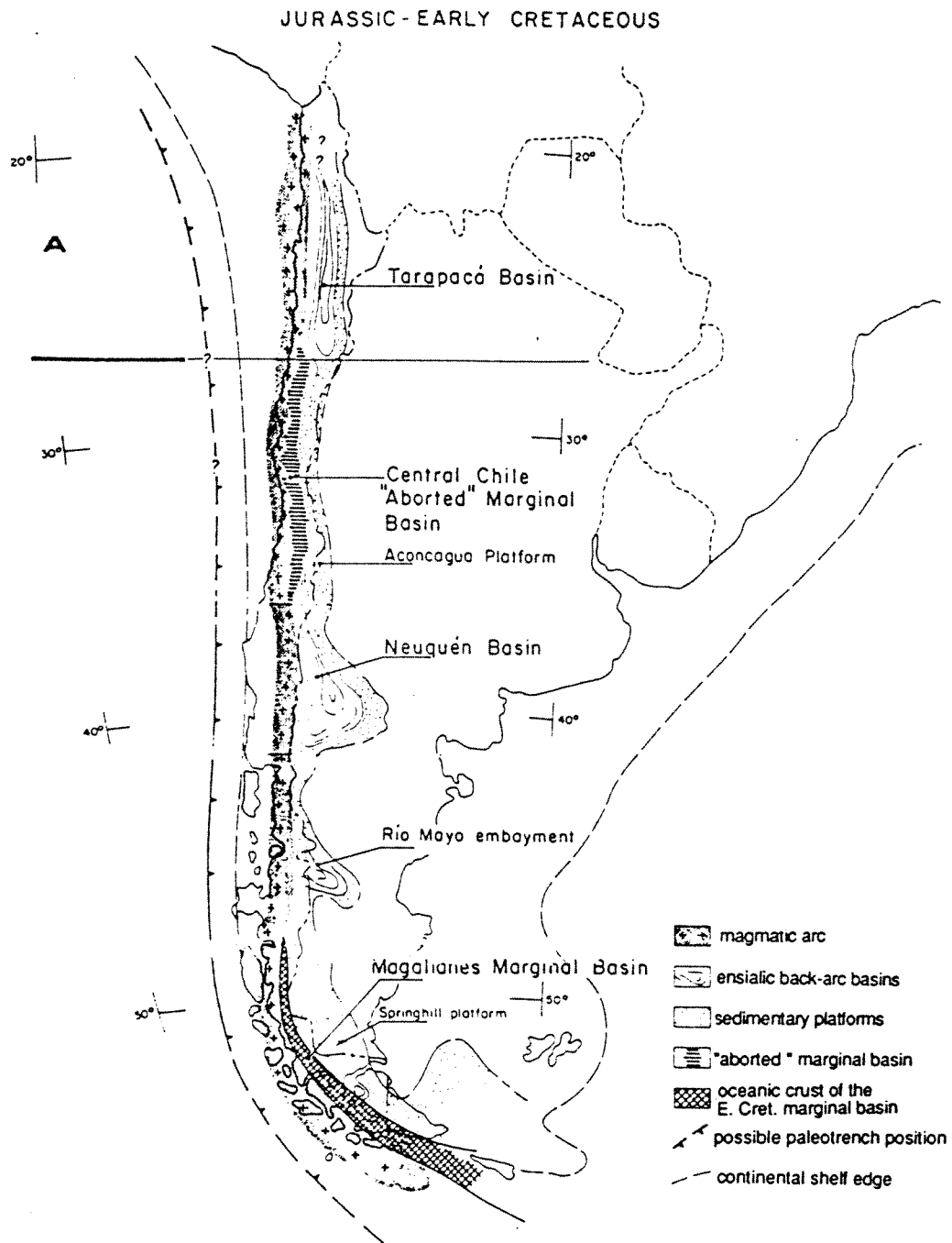


Figure 3. The Jurassic-Early Cretaceous arc back-arc basin systems of the Central and Southern Andes. Segment A is the area of the present study. (From Mpodozis and Ramos, in prep.)

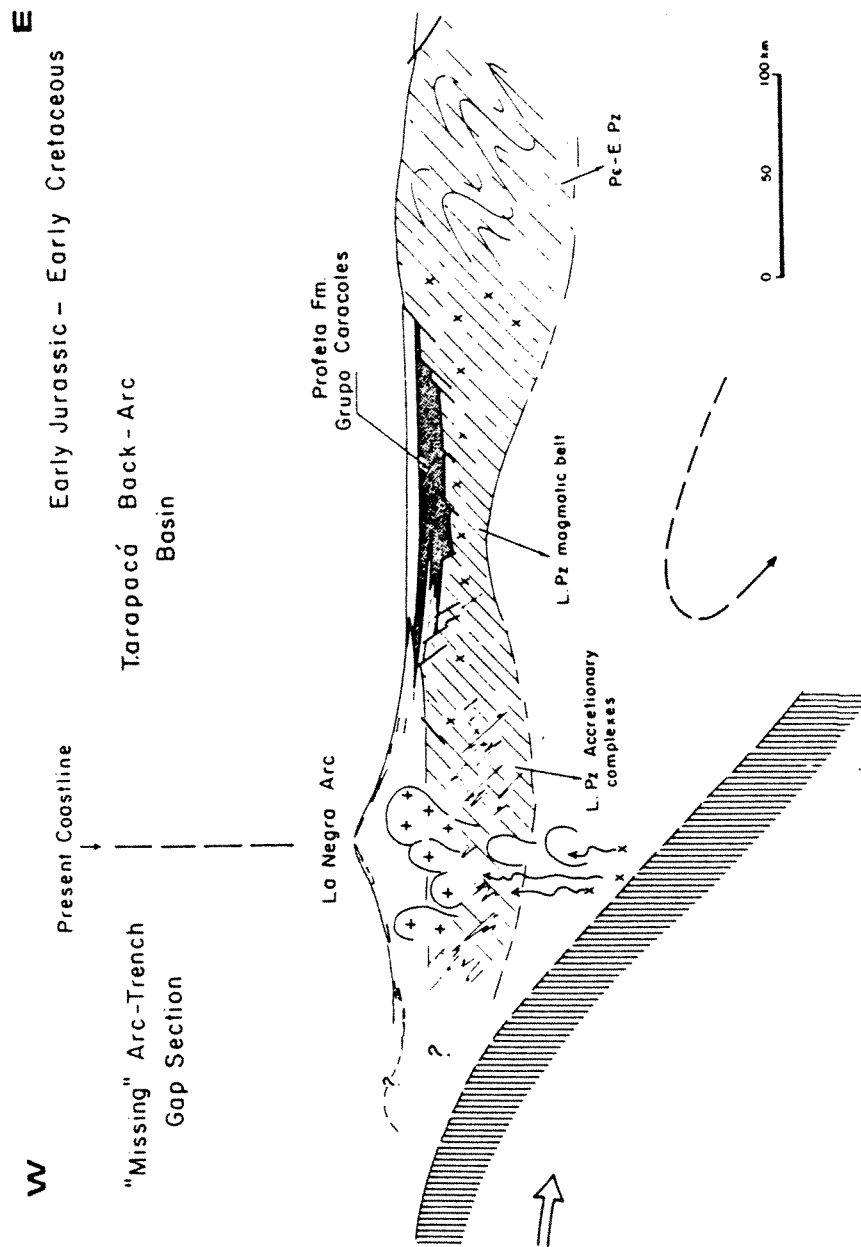
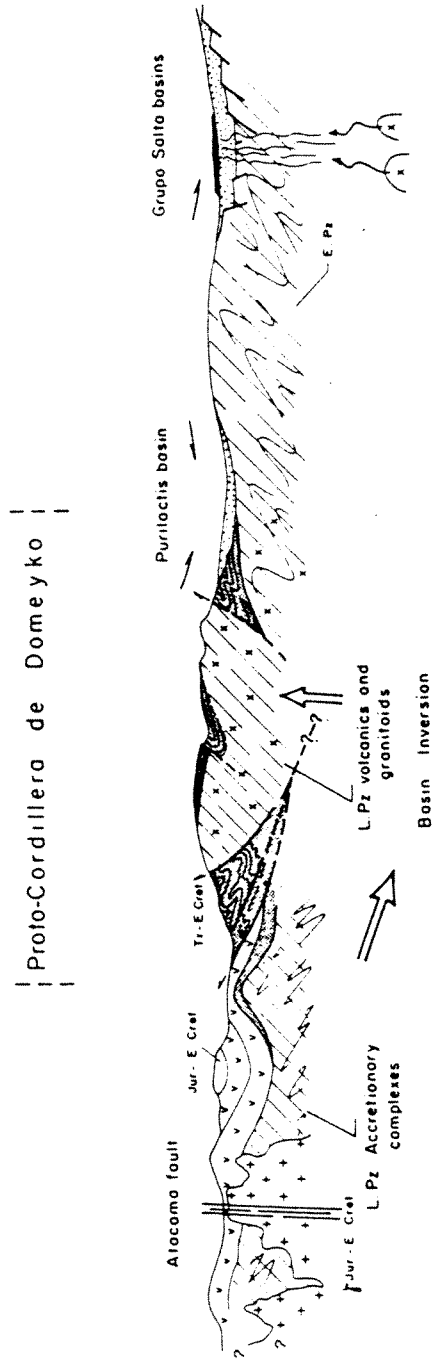


Figure 4. The Jurassic-Early Cretaceous magmatic arc back-arc basin in northern Chile. (from Mpodozis and Ramos, in prep.)

Magmatic activity ceased in the La Negra arc in the Middle Cretaceous and the whole Andean domain was deformed. The back arc basin was uplifted and thrust between the inactive arc and the foreland margin (fig. 5) and became a positive topographic element called the proto Cordillera de Domeyko. The sediments eroded from this element were deposited into basins to the east.

During the Latest Cretaceous, the axis of volcanism moved eastward and became established between the Coastal Ranges and the proto-Cordillera Domeyko. This volcanism lasted until the Eocene, and is represented by the Augusta Victoria and Azabache Formations (Ferraris and DiBiase, 1978). There is evidence of some magmatic activity occurring in the Cordillera de Domeyko during the Oligocene. Here, the north-south alignment of the large porphyry coppers of the Atacama Desert have been dated from 48 to 28 Ma. (Boric et al, 1985) and appear to have been emplaced through a younger and more eastern longitudinal fault than the Atacama Fault Zone. This magmatism is correlated with a period of highly oblique convergence between the Nazca and South American plates (Cande, 1983).

In the Late Oligocene-Early Miocene, the deformation of Cordillera de Domeyko, the folding of Late Eocene-Oligocene sediments, and the reactivation of reverse faults all occurred (Mpodozis and Ramos, in prep.). These orogenic effects have been noted by Mpodozis and Ramos (in prep.) to have occurred concurrently with a second change in the



Late Cretaceous

Figure 5. Cross-section of northern Chile (21°-27°) in the Middle Cretaceous.
(from Mpodozis and Ramos, in prep.)

relative motion of the Nazca and South American plates that resulted in a increased component of convergence (Cande, 1983). The axis of volcanism continued its eastward migration into the Western Cordillera in the Early Miocene. This progressive eastward migration through time is illustrated in figure six.

The specific structural history of the Coastal Cordillera in the region of the sampling sites is dominated by its history of high angle block faulting. This is conceptually linked by most workers to the history of the Atacama Fault Zone. In addition to the faulting, the Mesozoic bedded sequences in places are also affected by gentle folds with NNW-SSE axial trends (Ferraris and DiBiase, 1978). However in general, these sequences in the eastern part of the Coastal Cordillera have a monoclinial structure with N-S strikes and very gentle westward dips.

The Atacama Fault Zone is one of three major longitudinal fault zones along the coast of Chile (fig. 7). At the present time, there has not been a detailed structural analysis of the fault zone directly in the study area. The faults continuity along strike argues that studies from other areas and general findings would be applicable. In general, the fault zone is believed to have played an important, if not dominate, role during the Late Tertiary and Quaternary in the morphologic development of the Atacama Desert (Mortimer, 1980). During this time period, its primary role was to vertically displace the Coastal Cordillera cutting off

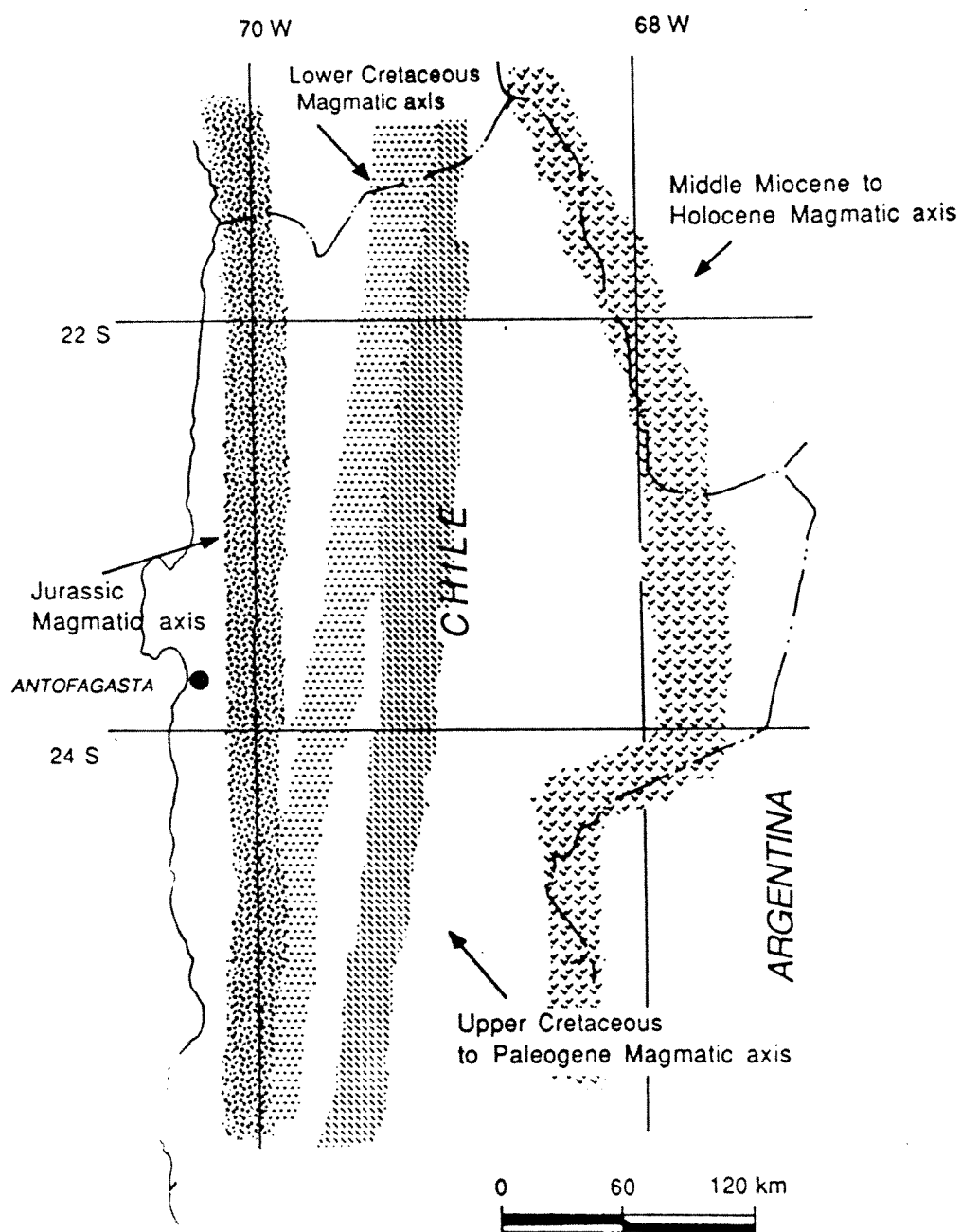


Figure 6. Map view of the axes of magmatism in northern Chile from the Jurassic until the present (from Makshev, 1984)

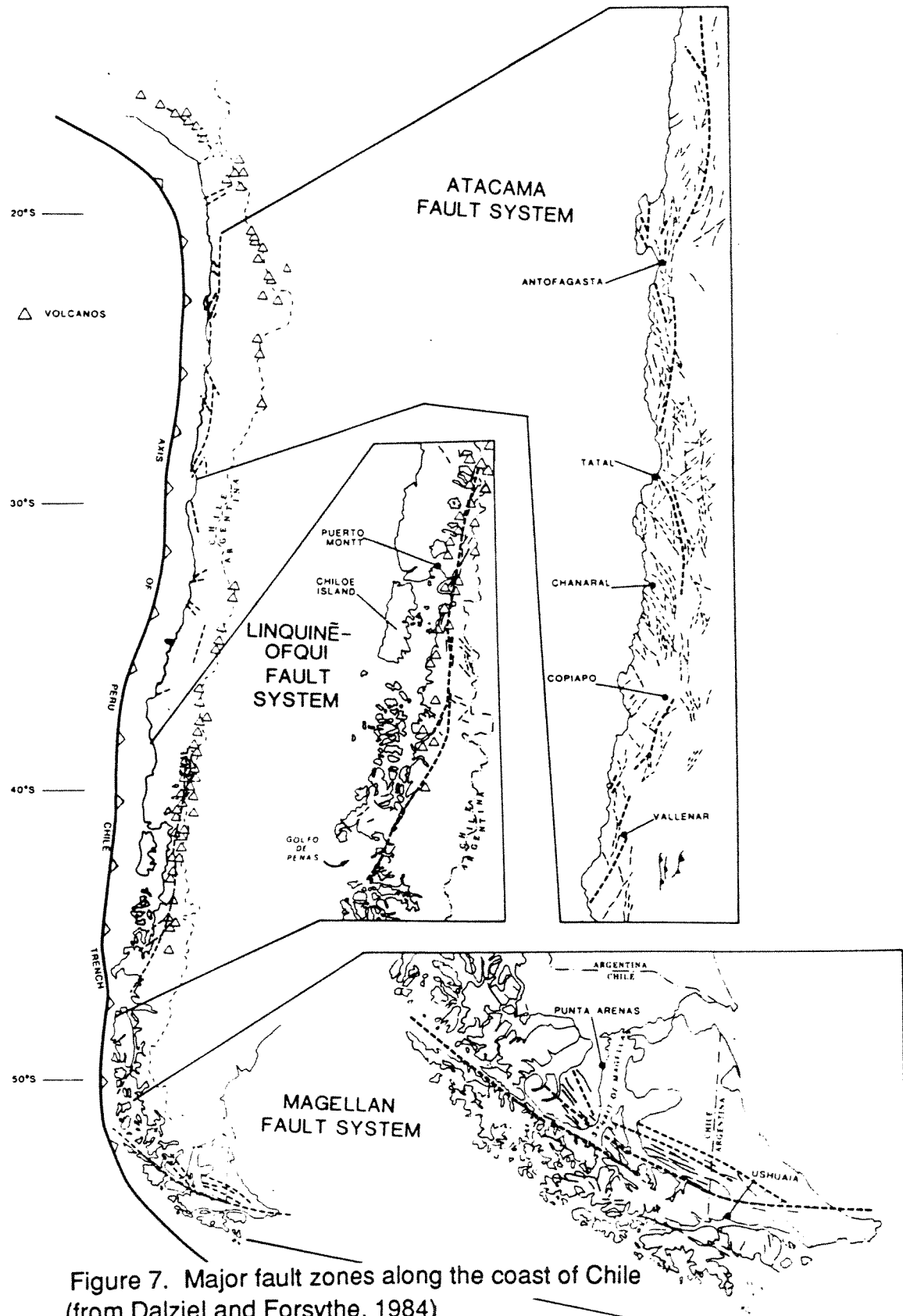


Figure 7. Major fault zones along the coast of Chile
(from Dalziel and Forsythe, 1984)

drainage patterns that once provided outlets directly to the sea (Mortimer, 1975). This late stage history of faulting has been generally assumed to be of normal fault character (Ferrasis and DiBiase, 1978). To the south of the study area between 25°-28°S, workers have documented major zones of subvertical mylonite belts (e.g. Naranjo et al., 1984). This evidence, together with other regional evidence for right-lateral displacements (e.g. Allen, 1965; St. Armand and Allen, 1960), has argued for an earlier period of right lateral strike-slip activity. The degree of strike-slip movement is qualitatively constrained by the fact that paleogeographic models document longitudinal and latitudinal coherence of the Jurassic and Cretaceous marine and nonmarine facies along and across the fault zone (e.g. Mpodozis and Ramos, in prep.). That is to say that this coastal block is not likely to be an exotic terrain. The mylonites themselves are cut by late stage veins that have been dated with K/Ar to be Neocomian in age (Naranjo et al., 1984). Also south of the study area, the fault is the locus of iron mineralization that has been stratigraphically constrained to be Cretaceous to Early Tertiary in age (Thiele and Pindreira, 1984). Thus, it has been argued that the fault zone had its beginnings, and perhaps most of its significant strike-slip activity, early on in the Cretaceous.

PALEOMAGNETIC TECHNIQUE

A gas powered drill was used to collect field cores approximately 2.5 cm. in diameter. The sampling sites were in Jurassic to Cretaceous plutons that were located in the Coastal Ranges of the Andes in Northern Chile, just south of Antofagasta, between latitudes 24° and 25°S (fig. 2). The sampling sites were located on both sides of the Atacama Fault Zone. The individual cores were oriented with aluminum orienting device to which a Brunton compass was attached. At Rutgers University, New Brunswick, weathered ends were removed with a rock saw and at least one specimen approximately 2.2 cm. long was cut from the original specimen.

After the Natural Remanent Magnetizations (NRM) of the specimens were measured, they underwent a progressive alternating field (AF) demagnetization of at least ten steps, but up to fourteen steps, using the Schonstedt GSD-1 AC Geophysical Specimen Demagnetizer located at Rutgers University, New Brunswick. Demagnetization began with five millitesla (mT) and generally ended at 90 mT but varied depending on the individual sample. After a sample started the demagnetization process, it was kept in a field-free shield. A flux-gate Molyspin spinner magnetometer, also located at Rutgers University, was used for all magnetic measurements. A few samples also underwent additional demagnetization using a Schonstedt TSD-1 Thermal Specimen

Demagnetizer.

Demagnetization techniques are important tools that help identify and remove secondary magnetizations which generally have lower stability than the primary magnetization (Collinson, 1983). In the AF demagnetization technique, the specimens are subjected to a peak alternating magnetic field which is intended to progressively decrease the remanent magnetization by increments to zero. In this way, the samples are taken through hysteresis loops of decreasing amplitude so that magnetic grains or domains with coercivities lower than the peak value are randomized (McElhinny, 1973; Collinson, 1983). This technique uses a series of progressively increasing peak values, a series of steps, to try and isolate different components of the magnetization history of the specimen. When there is stable magnetization that has a constant direction for a number of steps and this direction is common among a large number of samples it is called a "characteristic direction" (Dunlop, 1979). At each step, the specimen is rotated along three perpendicular axis so that demagnetization does not occur preferentially in one direction.

The thermal demagnetization technique utilizes the relationship between the relaxation time of magnetization and temperature-blocking temperature. A group of samples are heated at a series of temperatures, at each step the samples are cooled in a field free space and then measured. The magnetic grains with lower blocking temperature than the

temperature used will be randomized and the primary component of higher stability can be isolated.

Both demagnetization techniques have advantages and disadvantages that need to be considered when planning a paleomagnetic study. The AF technique, for which the peak field value is approximately 100 mT, because of equipment limitations, works well when the remanent carrier is magnetite, but not very well when the carrier is hematite. This is because the maximum theoretical coercivity for magnetite is only 300 mT (Evans and McElhinny, 1969) while for hematite it is much higher. The thermal method can be helpful in identifying the magnetic carrier, or carriers, because the curie point of pure magnetite is 578°C and for pure hematite it is 680°C, though the addition of titanium to either mineral will lower their curie points. Other secondary magnetic carriers also have characteristic curie points which makes it possible to infer the magnetic carrier from the progressive thermal process. While the thermal demagnetization technique is useful in discovering the range of unblocking temperatures and the curie point, oxidation of magnetite to hematite can occur in the heating process of the furnace. So generally AF demagnetization is used when the primary carriers would be magnetite and titanomagnetite (igneous rocks) and thermal demagnetization is used when hematite is the primary carrier (red sedimentary rocks).

Preliminary samples were collected in the summer of 1985 from eleven sites. Four to eleven samples were collected from each site. These samples were measured and

underwent demagnetization as described above. Sites that gave promising, and some that gave not so promising, results were recollected during a return trip in the summer of 1988. Component analysis only took place after all samples from both trips had undergone complete demagnetization.

Magnetite is a primary mineral of plutonic rocks so these rocks were subjected to AF demagnetization to avoid the possibility of oxidation in the furnace of magnetite to hematite. Most of the samples responded well to this demagnetization method showing intensity decay to less than ten percent of original intensity. This further reinforces the hypothesis that main remanent magnetic carrier was magnetite since hematite does not respond well to the AF method.

A few samples did not show decay to less than ten percent of initial intensity with the AF demagnetization process though they did yield consistent results; these samples were subjected to additional thermal demagnetization. They dropped in intensity significantly at temperatures of 600°C to 625°C. Until the samples were exposed to these thermal steps, their declinations and inclinations were also stationary. The resulting changes in this temperature range were mostly viscous, though samples from site JPCA did show a resultant vector that mimicked a vector commonly observed during AF demagnetization of other samples. It could be possible that there was secondary alteration of some of the plutons. This could lead to oxidation of primary magnetite to

secondary hematite, and could have happened even during the initial cooling process. Since the observed unblocking temperature is much lower than the 680°C curie point for pure hematite, this may infer that the mineral is a titanohematite since a component of titanium lowers the curie point. There is another possibility that should be mentioned. The temperature gauge on the furnace may be at fault as has been the case in the past with the same furnace (R.Forsythe, per. comm.). This possibility was given more credibility when it was noticed this July that when the furnace gauge was set for 650°C, the temperature gauge was only reading 640°C a half hour later. There is no quick or easy way to test the possible malfunction of the furnace. I would argue that the alternating field method yielded the primary magnetite remanent magnetization components and that though there may possibly be a hematite alteration product in a few samples the alteration did not fully remove the primary magnetization.

COMPONENT ANALYSIS

After all cores had undergone the demagnetization procedure described above, the results were then plotted on Zijdeveld diagrams. These diagrams are orthogonal projections that combine intensity and directional changes of the data (Zijdeveld, 1967). The Zijdeveld plots of each sample were then inspected to isolate demagnetization segments which were in turn subjected to a three dimensional least squares, best straight line analysis (referred to by

some as principal component analysis). This was accomplished using an interactive computer program on the IBM PC adapted by Chris Jesinkey following original work by Kirschvink (1980). This general approach helped to locate and statistically define linear regions (i.e. individual magnetic components) of the data. By grouping common components from each sample within a site, mean directions were then calculated for each site according to standard paleomagnetic procedures (where the vectors for each individual component are regarded as points on a unit sphere) (Fisher, 1953). The statistical parameters of Fisher (1953) include a precision parameter (k) and an accuracy estimation (α_{95}). The precision parameter (k) determines the scatter of the directions, and as k becomes larger, the population is found to move more tightly around the true mean. The α_{95} value represents a "cone of confidence" around the calculated mean vector within which there is a 95% probability that the true mean direction is located. After determining the means and Fisherian parameters for each site, the means were used to calculate average directions for the region as a whole. Paleopoles were calculated from the overall mean declinations and inclinations using the axial geocentric dipole hypothesis.

PALEOMAGNETIC RESULTS

Samples from eleven sites were available for the paleomagnetic study. Six of the eleven sites yielded statistically sound results that could be used to calculate one or two characteristic directions for each site. Of the other five sites, two appear to represent lightning strike magnetism, two have magnetization too viscous or statistically erratic to be used in any confident manner, and for one site the labels on the cores became unreadable after shipping and a proper field correction could not be deduced. Five of the six coastal pluton sites that gave characteristic directions have been previously radiometrically dated and were found to range in age from 157 to 128 ma. (Mpodozis, written communication)

There were two common characteristic components in each of the six sites, a normal component and a reversed component. The normal component is very similar to the expected present day field, while the reversed component has a declination rotated significantly clockwise from the antipode of the the present day field. Looking at the samples individually it can be demonstrated that the normal component was generally removed under AF demagnetization with lower fields than the reversed components of the same sample (see fig. 8). A graph of the coercivity spectra for the samples as a group also demonstrates (fig. 9) the partial overlap of the two components and shows that the normal

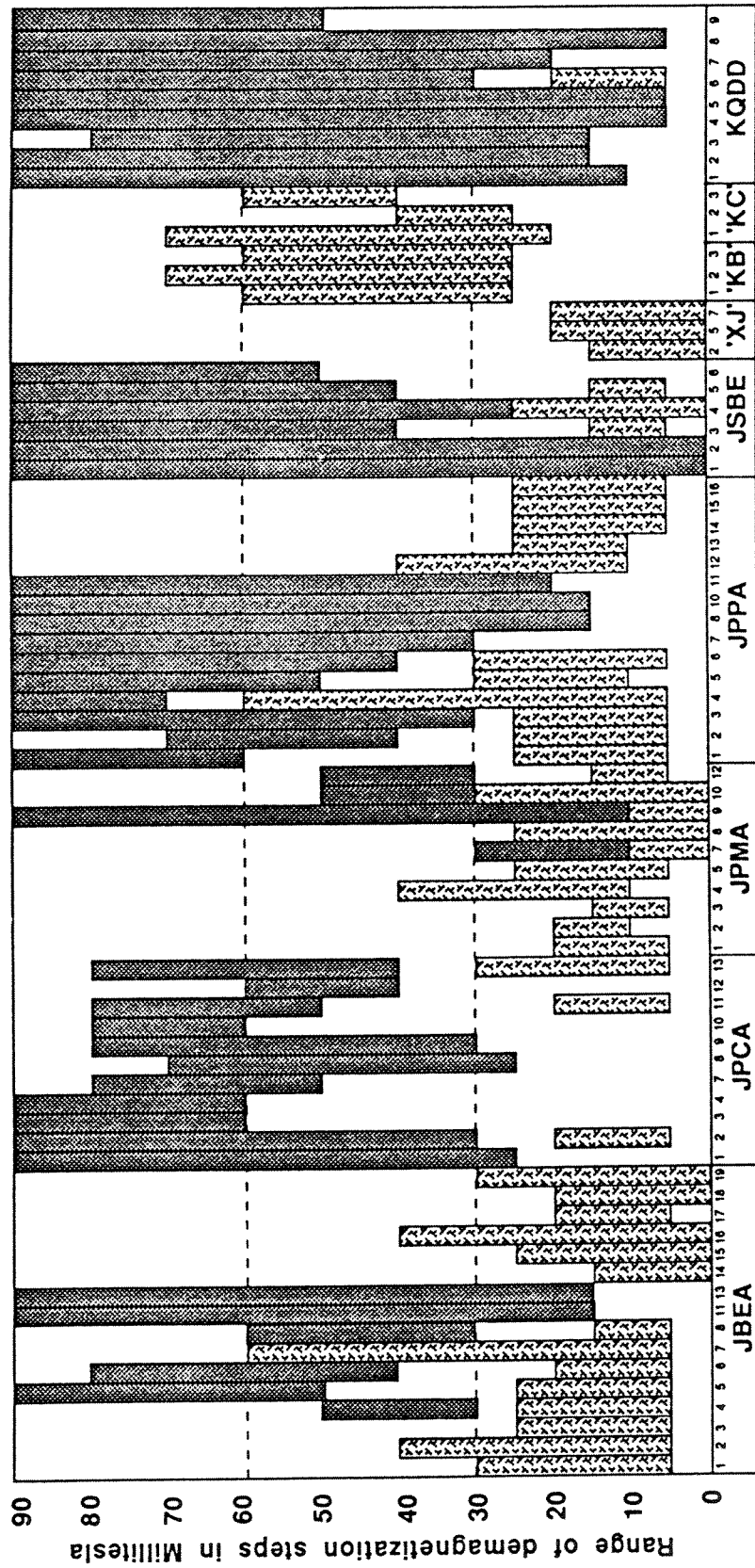


Figure 8. Bar graph demonstrates the coercivity range of the magnetic components isolated in each of the samples used to calculate the site mean directions in this study

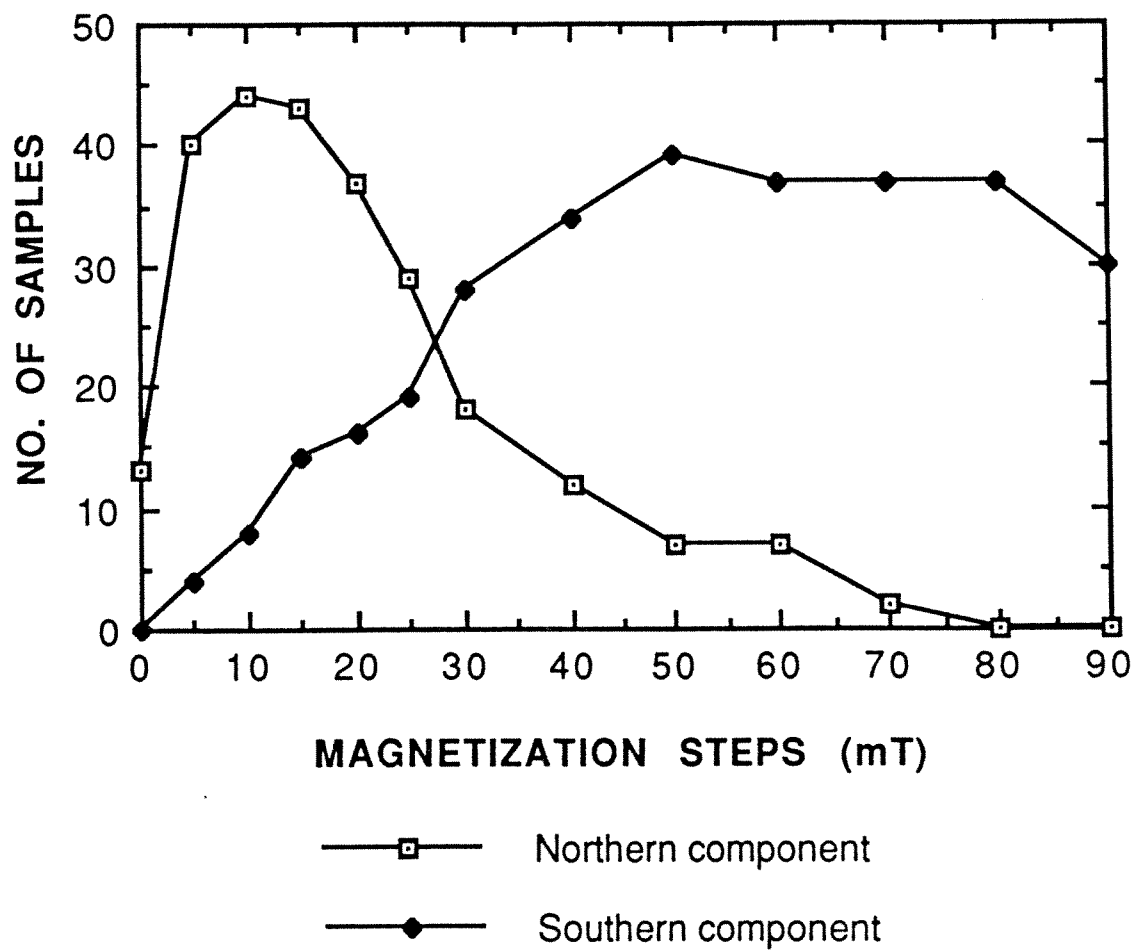


Figure 9. The coercivity spectra showing the partial overlap of the two magnetic components isolated

component is the lower coercivity secondary magnetization.

SITE JBEA

Eleven cores from site JBEA were drilled in the summer of 1985, and eight more were drilled in the summer of 1988. They were mostly granodiorite though a few were xenoliths and three were aplite. Of these nineteen cores, sixteen yielded consistent linear trajectories. Their intensities range from 20.02 to 0.38 mT with all but five between 6.7 and 3.2 mT. Samples were treated with AF demagnetization in twelve step (5,10,15,20,25,30,40,50,60,70, 80, and 90 mT) except for JBEA-1 and JBEA-3 which were only treated up to 70 mT because they exhibited viscous behavior after 40 mT.

Demagnetization yielded two components from this site. The normal field magnetization is very close to the present day field direction for the site with a mean declination of 358.3° , mean inclination of -49.3° , and α_{95} of 6.1° . The reversed field direction is rotated clockwise from the expected with a declination of 202.4° , inclination of $+37.8^\circ$, and α_{95} of 11.8° (table 1). Combined components are found in four samples (fig. 10a. and b.), reversed only components are found in two, and normal only components are found in ten samples (fig. 10c.). The normal direction is a low coercivity component generally found in the range of 5 to 25 mT while the reversed direction is the high coercivity component that usually takes over at 30 mT (fig. 8 and 9). In all but four samples, intensities decayed to less than ten percent of the original intensity.

Table 1. Paleomagnetic results from the Coastal Plutonic Complex

ROCK_UNIT	SITE	AGE	No	R_OR_N	DECLINATION	INCLINATION	k	alpha_95
Granodiorite w/aplite & zenol.	JBEA	157+4 Rb/Sr	15	N	358.3	-49.3	35.0	6.1
same as above	JBEA	157+4 Rb/Sr	6	R	202.4	+37.8	23.5	11.8
Granite	JSBE	UNDATED	6	N	4.8	-20.2	15.6	14.5
same as above	JSBE	UNDATED	6	R	216.0	+13.8	154.3	4.6
Gabbro w/granitic aplite dikes	JPPA	148+4 K/Ar	11	N	6.7	-33.9	24.9	8.5
same as above	JPPA	148+4 K/Ar	11	R	198.1	+34.7	41.7	6.5
Granite	JPPA	149+2 K/Ar	10	N	349.2	-33.2	17.8	10.5
same as above	JPPA	149+2 K/Ar	4	R	193.6	+45.0	17.7	16.6
Gabbro	JPCA	150+5 K/Ar	3	N	357.2	-41.1	9.8	25.8
same as above	JPCA	150+5 K/Ar	11	R	202.6	+36.6	21.2	9.2
Monzogranite	KQDB-C-D	128+3 K/Ar	7	N	28.2	-49.8	20.7	11.6
same as above	KQDB-C-D	128+3 K/Ar	9	R	229.9	+31.0	67.5	5.7

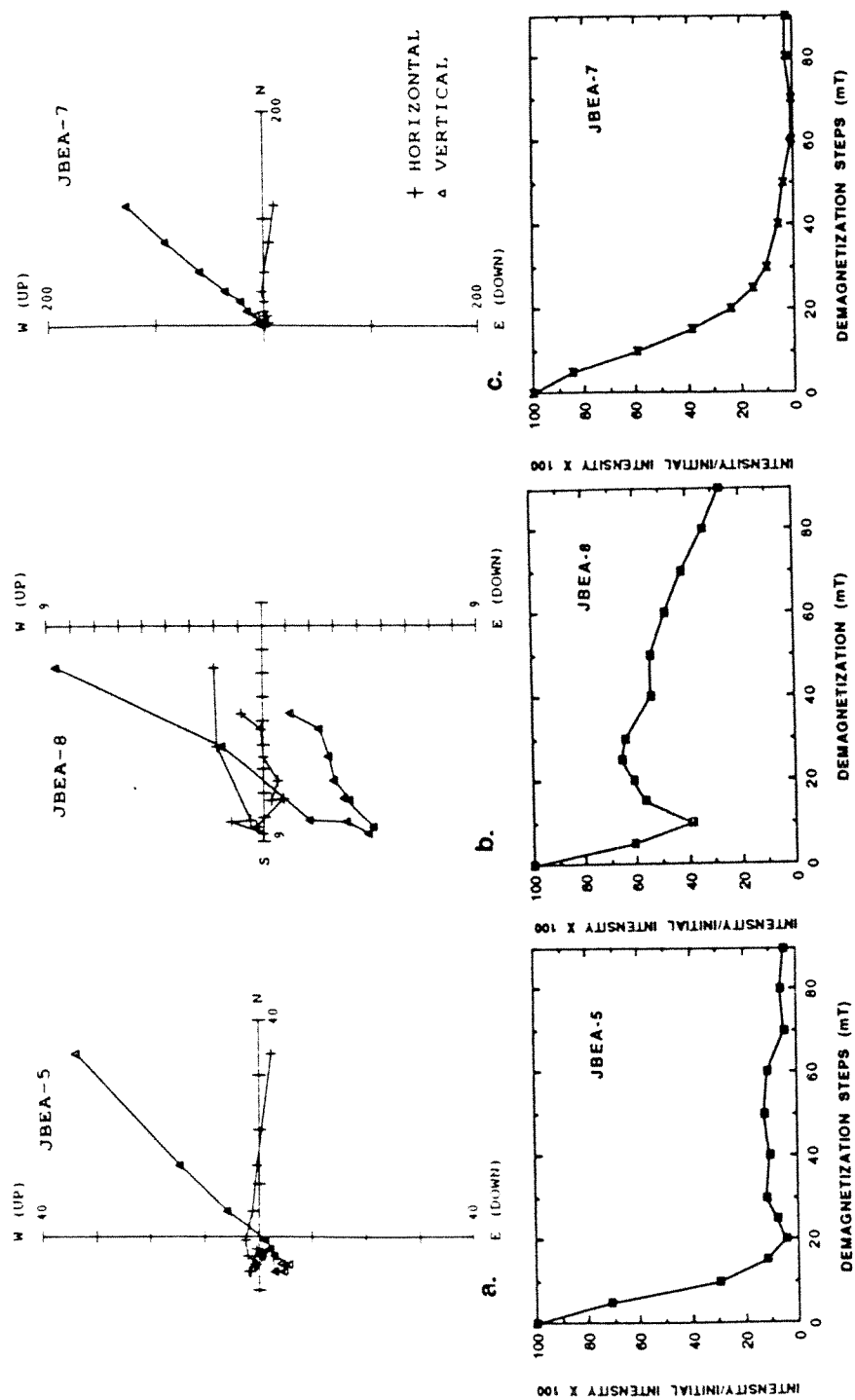


Figure 10. Typical Zijdeveld and J/J_O plots of samples from site JBEA. a. with both components the J/J_O plot shows an increase in intensity when the reversed component is revealed. b. with both components, the J/J_O plot shows an increase in intensity when the reversed component is revealed. c. with the normal component only, the J/J_O plot shows no increase in intensity.

The intensity/initial intensity plots give an indication of the number of components that an individual sample reveals. Samples JBEA-5 and JBEA-8 have both the normal and reversed component and their J/J_0 plots show an increase of intensity where the reversed component starts to be revealed (Fig. 10a. and b.). Some of the JBEA samples only yield the normal component and they do not show the increase in intensity (fig. 10c.). Similarly, samples that only yield the reversed component do not show the increase in intensity except in the very low coercivity range. There might also be a low coercivity component in these samples but it can not be resolved with the paleomagnetic method.

SITE JSBE

All of the thirteen cores obtained in 1985 and in 1988 at site JSBE were granite. After they had undergone a twelve step AF demagnetization treatment from 5 to 90 mT, stable and consistent components were isolated in nine samples. The sites mean normal magnetization declination is 4.8° , inclination is -20.2° , and α_{95} is 14.5° . The mean reversed direction declination is 216.0° , inclination is $+13.8^\circ$, and α_{95} is 4.6° . The NRM intensities ranged from 14.68 to 2.53 mT. Six samples had reversed direction trajectories that decayed towards the origin (fig. 11a.). In three of these, only the reversed component was present while the other three samples also had the low coercivity normal component (fig. 11b.). Three other samples had good trajectories in the northerly and up direction (fig. 11c.).

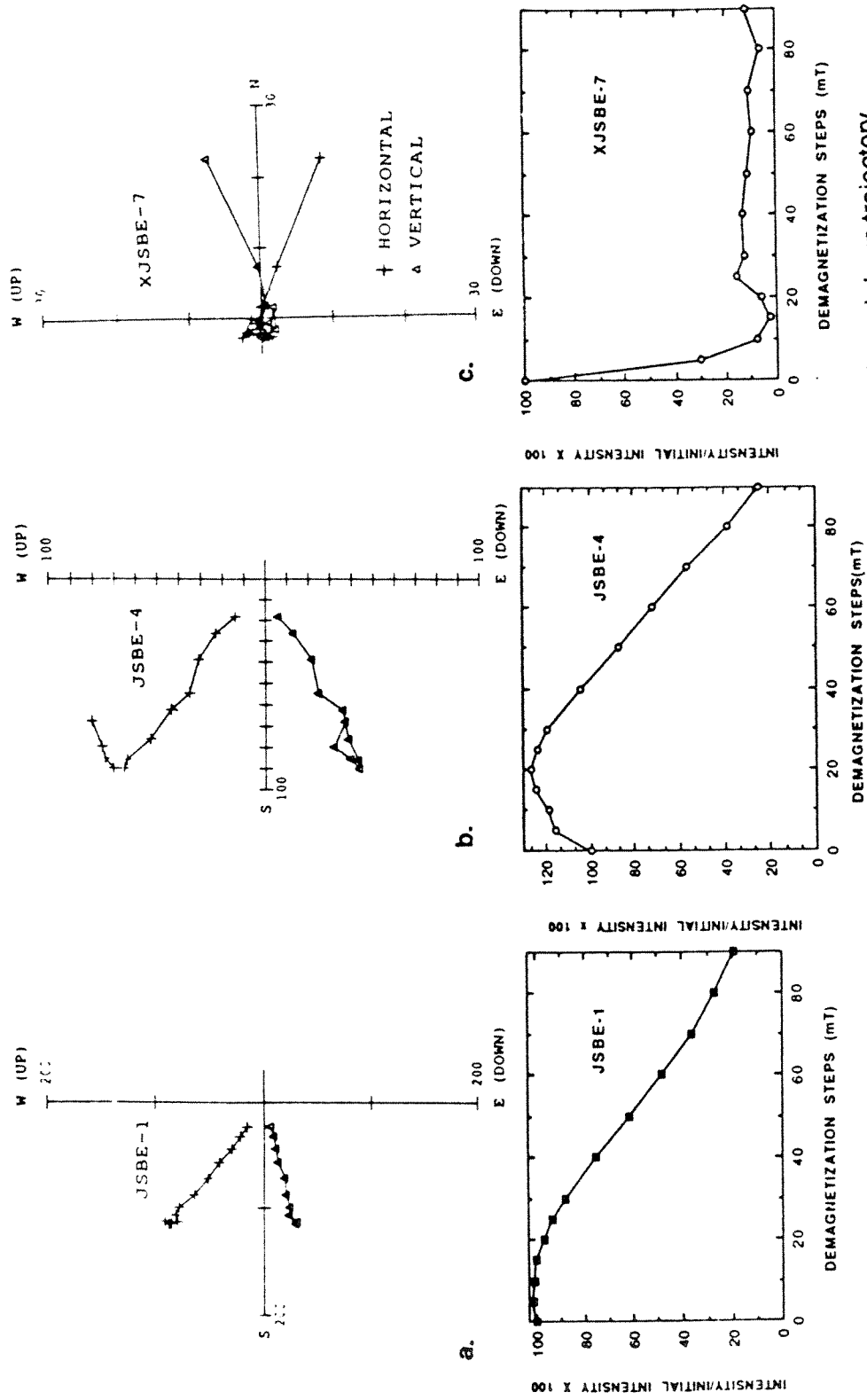


Figure 11. Typical Zijderveld and J/J_0 plots of samples from site JSBE a. with southerly and down trajectory b. with both the northerly and up and the southerly and down trajectories c. with the northerly and up trajectory

The coercivity ranges of the directions are 5 to 90 mT for the reversed direction and NRM to 25 mT for the normal direction.

None of the reversed field samples decay under AF demagnetization to less than ten percent of the NRM intensity. It can be argued that the NRM intensities do not accurately represent the original intensities in this case due to the presence of a secondary component with opposing polarity. An increase in intensity occurs as the opposing direction magnetization is removed so if the true initial intensity was used then the samples would show decay to closer to ten percent. This explanation appears to partially account for unusually strong intensities that are found in some of the samples even after they have undergone 90 mT cycle in AF demagnetization.

SITE JPPA

Of the seventeen cores drilled from site JPPA, eleven were gabbro and six were aplite. Cores were collected during both the 1985 and the 1988 trips. The samples underwent a twelve step AF demagnetization from 5 to 90 mT. Statistical component analysis was carried out on fifteen samples after two were discarded on the basis of lacking any resolvable characteristic magnetic components. Both the normal and the reversed directions were isolated in six samples (fig. 12a.), five samples only revealed the normal component (fig. 12b.), and four samples only revealed the reversed component (fig. 12c.). The normal component has a site mean declination of

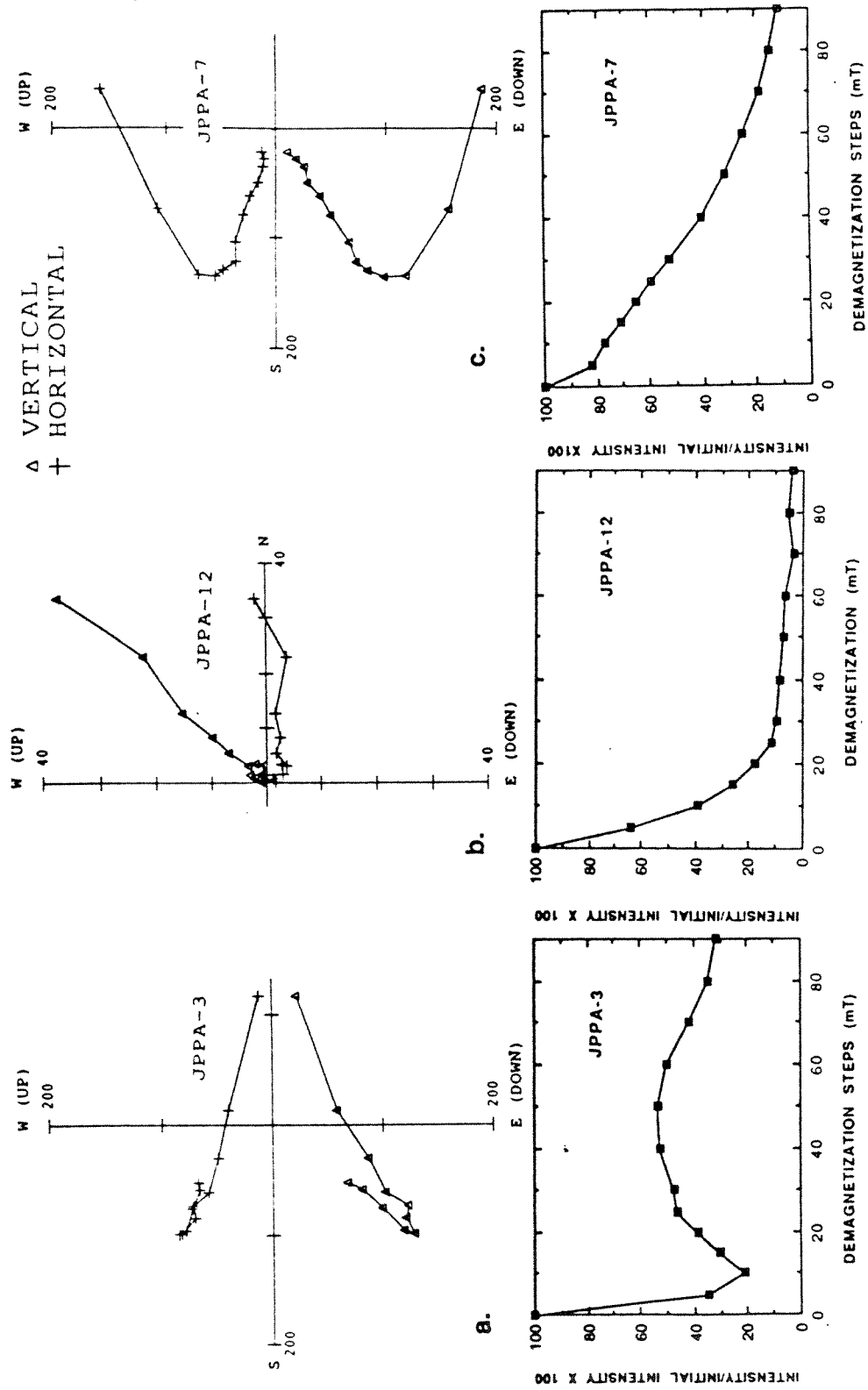


Figure 12. Typical Zijdeveld and J/J_0 plots of site JPPA a. with both components b. with the normal component c. with the reversed component

6.7°, inclination of -33.9°, and alpha 95 of 8.5°. The mean for the reversed component is declination 198.1°, inclination +34.7°, and alpha 95 of 6.5°. The coercivity ranges for this site are very similar to the previous sites. The normal direction range is 5 to 60 mT with most of the samples lower than 30 mT, and the reversed direction range is 15 to 90 mT.

This site also had the decay dilemma discussed above. When the sample only had the low coercivity normal component, the intensities show the normal decay of magnetite exposed to AF demagnetization. Sample JPPA-3 underwent additional thermal demagnetization in ten steps (100-625°C) and the intensity dropped off significantly between the temperatures of 600 and 625°C though the technique only yielded spurious results (fig. 13).

SITE JPMA

Half of the twelve granite cores from JPMA were collected in 1985 and the other half were collected in 1988. Ten of these samples yielded coherent trajectories under AF demagnetization. The mean of the ten samples with the normal component is declination of 349.2°, inclination of -33.2°, and alpha 95 of 10.5°. Four of the samples also yielded the southerly and down component with a mean declination of 193.6°, mean inclination of +45.0°, and alpha 95 of 16.6°. The NRM intensities range from 10.86 to 1.96 mT with all but one below 6.5 mT. In this set of samples, the coercivities of the two components overlap more than at other sites. The normal magnetization range is NRM to 40 mT and the reversed

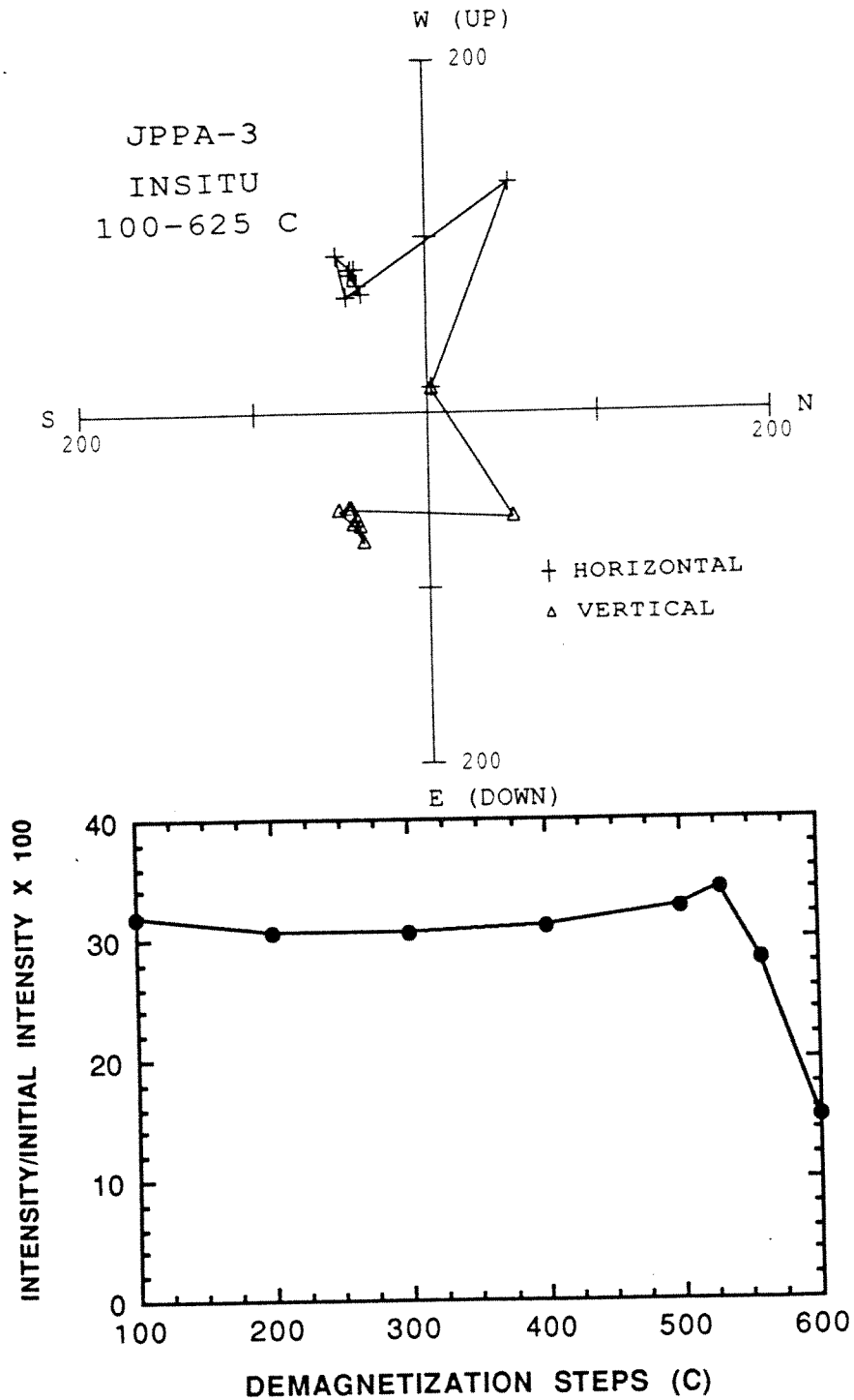


Figure 13. Zijderveld and J/J_0 plots of JPPA-3 after undergoing additional thermal demagnetization .

range is from 10 to 90 mT. All but one sample decayed to less than 12.5 percent using twelve steps of AF demagnetization from 5 to 90 mT. Figure 14a. shows the typical response of this sample set to AF. The rounded, two component zijderveld of figure 14b. is one way to predict the somewhat overlapping coercivities found in all of the two component samples (Collinson, 1983 p.371).

SITE JPCA

Site JPCA was also visited both summers to drill a net of eleven gabbro cores. All eleven samples yielded well defined southerly and down directions in the 25 to 90 mT range when exposed to a twelve step AF demagnetization (5 to 90 mT). Three samples also had good northerly and up directions in the 5 to 30 mT range with a mean direction declination of 357.2° , inclination of -41.1° , and alpha 95 of 25.8. The reversed component had a mean declination of 202.6° , mean inclination of $+36.6^\circ$, and alpha 95 of 9.2° .

Most of the samples show relatively straight forward decay under AF cleaning (fig. 15.), but three samples (fig. 16a.) did not even decay to less than 40 percent, though in the last four to five steps they did yield the reversed component (fig. 16b.). These samples underwent additional thermal demagnetization from 100° to 625°C in nine steps. At 530°C they showed as slight increase in intensity and then there was steady decay until 625°C where there was a significant decrease in intensity (fig.16c.). From the

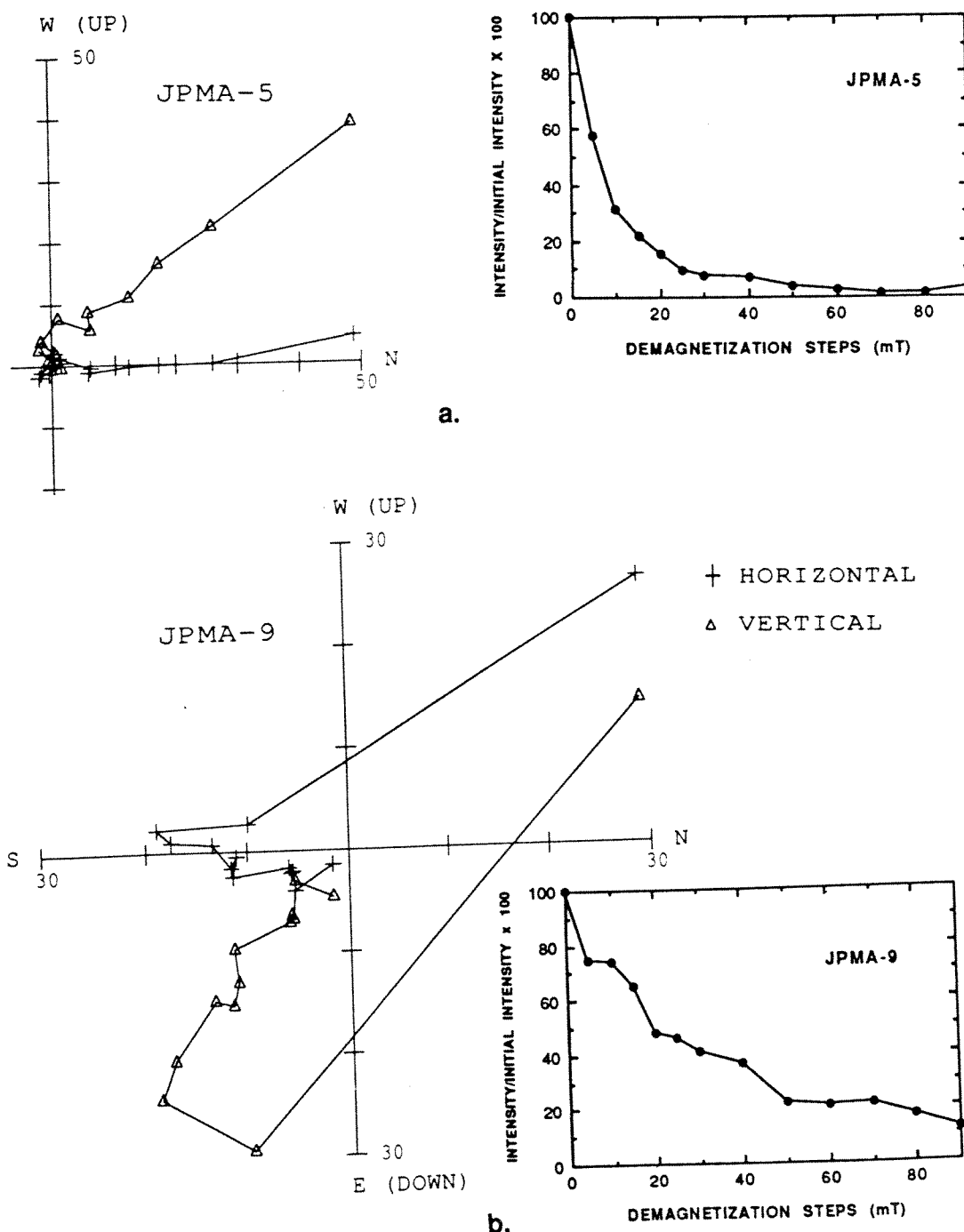


Figure 14. Typical Zijderveld and J/J_0 plots of site JPMA
 a. with the normal component isolated b. with both components isolated, the rounded intersection between the two components is characteristic when the components coercivities overlap somewhat

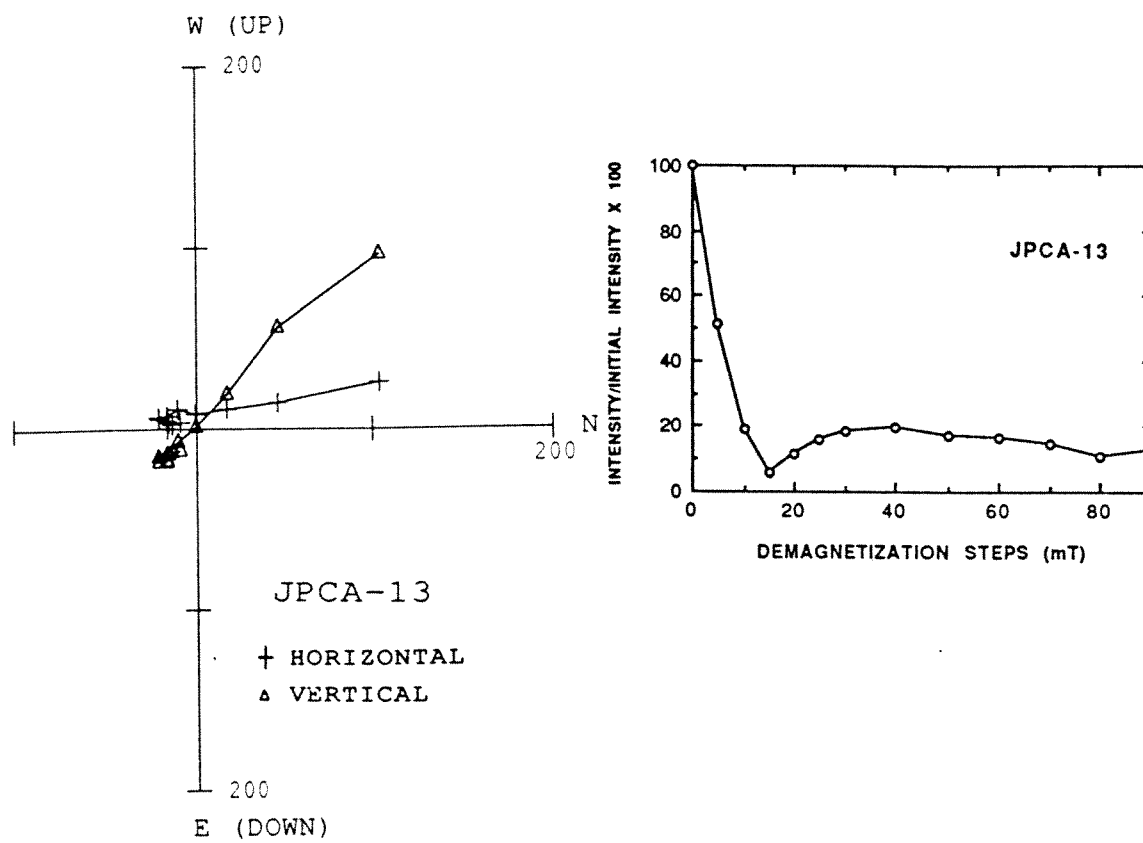


Figure 15. Typical Zijderfeld and J/J_0 plots of site JPCA

Zijderveld plots (fig.16d.) it can be noted that at the same step the vector projections, which had not moved since the heating had begun, also started decaying into the origin in the same southerly and down direction.

If the furnace is calibrated correctly then there could be a component of hematite in the magnetization of these samples along with the magnetite. The decay of remanence under AF is uncharacteristic of hematite, but the remaining remanence above 580°C suggests the presence of titanohematite. Since the vector is in the same direction for demagnetization processes, there are a few possibilities. Either the magnetite is primary and the hematite was an oxidation product occurring during the cooling of the pluton early on or both were remagnetized at a later date perhaps due to its proximity to a cross cutting younger pluton.

SITE KQDA-D

The Cretaceous pluton of site KQDA-D is a monzogranite; here nine samples were collected during each summer. Of all the sites in this study, this one is the only one on the east side of the fault that gave good results, it is the youngest, and it is closest to the fault. The NRM intensities range from 484.33 to 3.58 mT. Samples underwent AF demagnetization in ten or twelve steps. Three of the eighteen samples were rejected because they had inconsistent directions. All of the rest of the samples responded well to AF cleaning, and all but one decayed to less than ten percent of initial

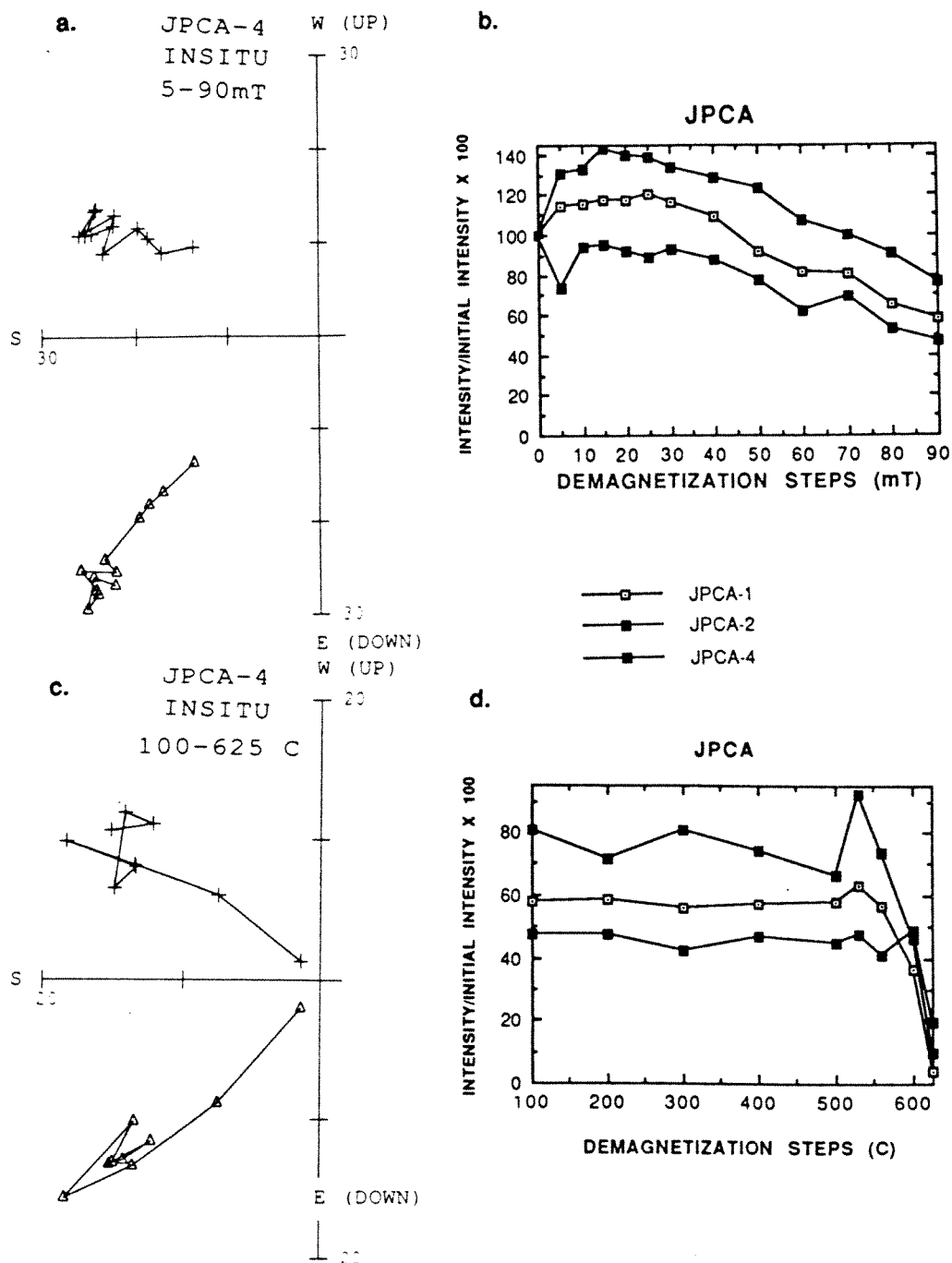


Figure 16. a. Representative Zijderveld plot of samples JPCA-1,2,4 under AF demagnetization b. J/J_0 plot showing the samples' response to AF demagnetization c. Representative Zijderveld plot of samples under thermal demagnetization d. J/J_0 plot showing the samples' response to thermal demagnetization (see text for discussion)

intensity.

This set has both a normal and a reversed component similar to the other sites, but the coercivities of the directions overlap completely. Seven samples only have the northerly and up direction in the range of 20 to 70 mT (fig. 17a.). Nine samples have the southerly and down direction in the similar range of 5 to 90 mT (fig. 17b.). Only one of the samples has both directions, a small normal component from 5 to 20 mT. Not only is the coercivity greater for these samples normal components (fig. 8 and 9), but it also is rotated clockwise from the present day magnetic field. These two factors make the normal component from this site a prime candidate for being antipodal to the reversed field instead of being a secondary present day field (see discussion section).

LIGHTNING STRIKES

The sites on the eastern side of the Atacama Fault were at a higher elevation than the sites on the western side, where the Pacific Ocean had exposed outcrop at sea level. Two out of three sites at higher elevations appear to have been remagnetized by lightning strikes.

Characteristics of lightning strike magnetization include large intensity values, random directions, and low coercivity magnetization (McElhinny, 1973; Piper, 1987). Lightning strikes have currents of 10^4 to 10^5 amps (McElhinny, 1973). After they strike, they spread out in a circular path and the intensity decreases away from

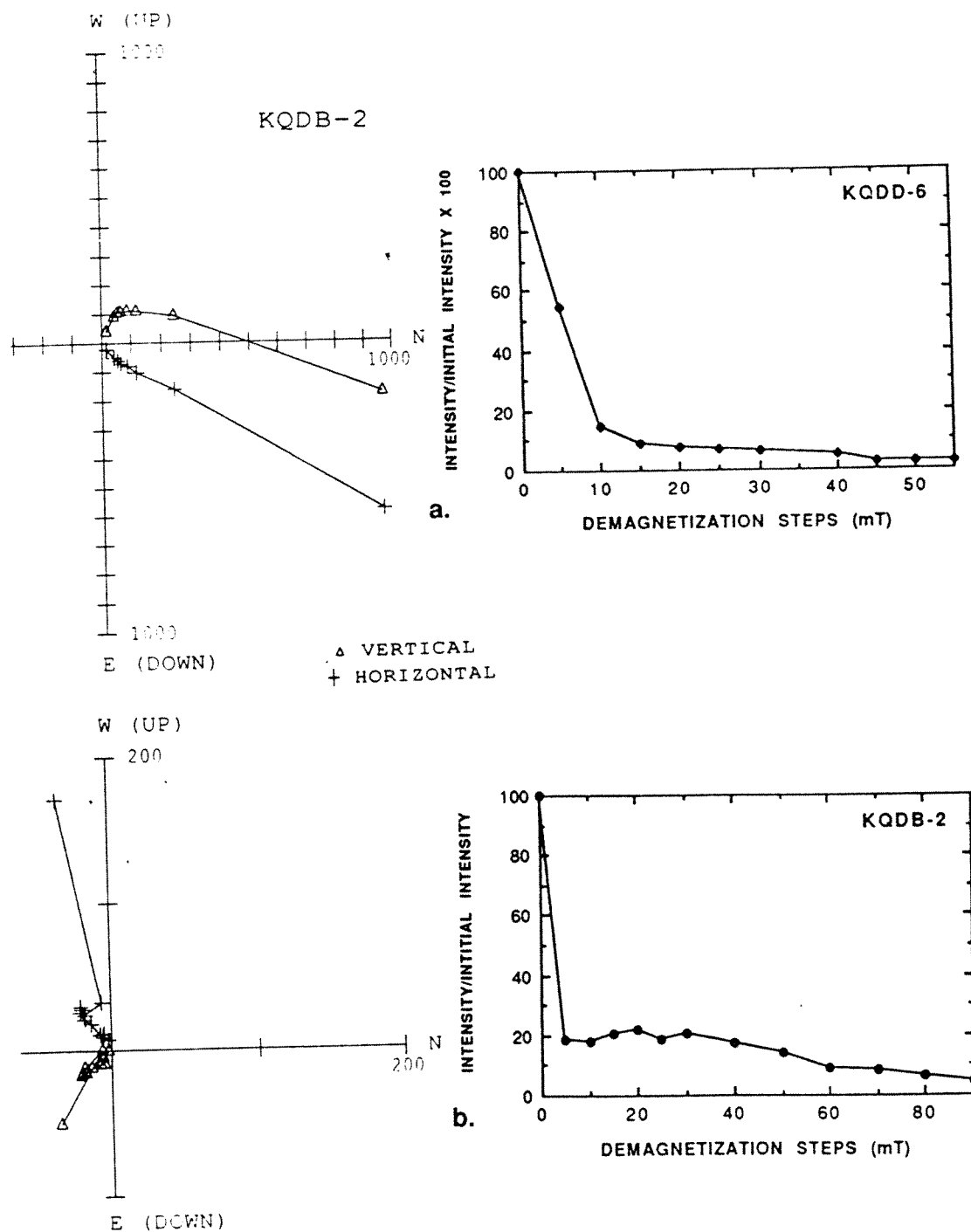


Figure 17. Typical Zijderveld and J/J_0 plots of samples from site KQDA-D
 a. with the normal component b. with the reversed component

the strike. Sites KSVM and KCCA demonstrate the characteristics of lightning strike magnetization.

The initial intensity of KSVM samples range from 5756.2 to 179.38 mT which at the low end is on the average of an order of magnitude higher than the rest of the normal samples and at the high end is more than 10^2 greater. This fact alone is not necessarily significant, but when the Zijderveld plots are compared it becomes obvious that while the plots show perfect univectorial decay towards the origin, practically every sample exhibits a different direction (fig. 18). This occurred in samples collected in both trips even though different areas of the pluton were sampled to try and avoid the lightning affected rock. Plots of intensity verses initial intensity (J/J_0) demonstrate the low coercivity of the samples (fig. 19). All twelve samples have less than ten percent of original intensity after being exposed to a 40 mT magnetic field; all but one sample has decayed to less than one percent at 70 mT.

Three other samples drilled during the resampling trip of 1988 at the KSVM site do not demonstrate the above characteristics. Their intensities are not as high; they range from 87.59 to 66.34 mT. They also all yield the same characteristic direction which possibly could be similar to the present day field found in other samples. The problem is that there are only three samples collected relatively close together therefore it is not clear whether they represent

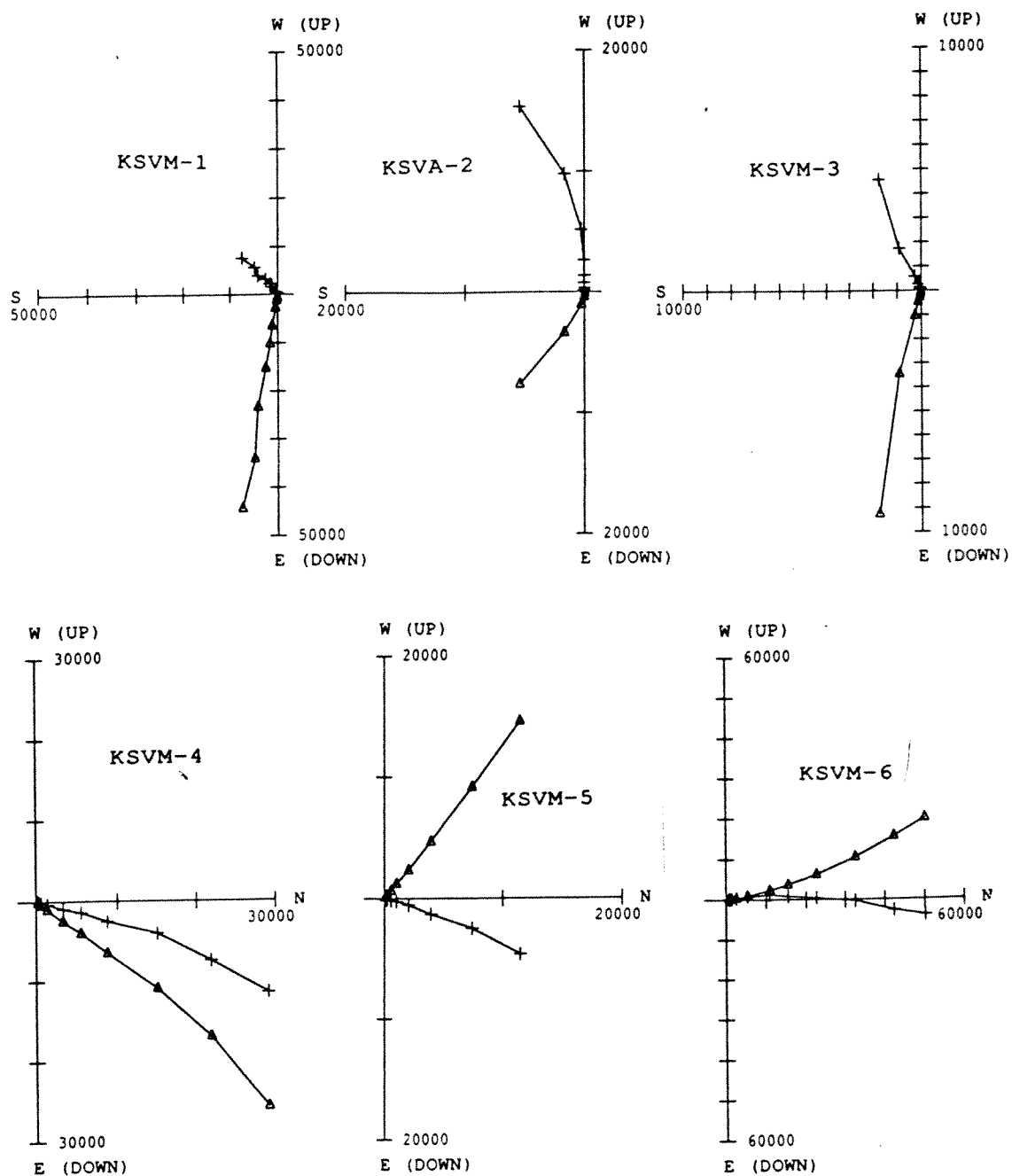


Figure 18. Zijdeveld plots of six of the original samples from site K SVM. Note the wide range of magnetic directions, a characteristic of lightning strikes.

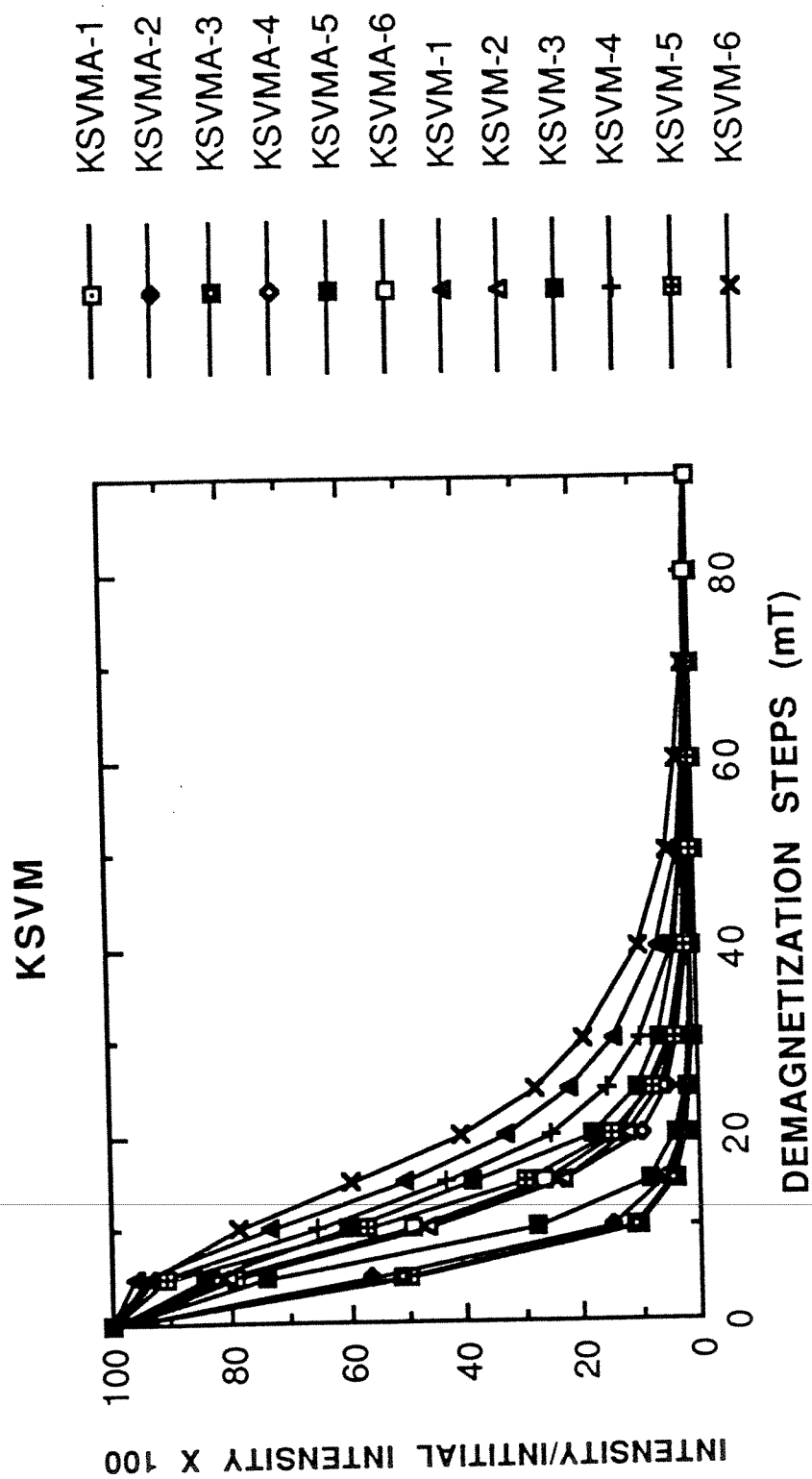


Figure 19. J/J_0 plots of twelve of the samples demonstrating the low coercivity

true natural remanent magnetization or a coherent zone within the area affected by a lightning strike.

Site KCCA is located on the western side of the Atacama Fault, but was also found at higher elevations. This sampling site showed similar characteristics to the KSVM site. The initial intensity range is not as high as the KSVM samples, the 692.55-53.92 mT range overlaps with other samples not affected by lightning, but the other typical characteristics are present. Most importantly, the samples decay univectorially to the origin, but there is not a statistically consistent direction (fig. 20). The coercivity of these samples is even lower than that of the KSVM site; all samples decay to less than ten percent of initial intensity after being exposed to only twenty-five mT (fig. 21). This site was not resampled on the return trip in the summer of 1988 because the road that lead to the site had been washed away when the rare event of rain triggered mud slides.

It is generally expected that lightning strikes can be avoided by drilling several samples several meters apart or by drilling deeper since they are a surface phenomena. In the Atacama desert, it is not that easy. Outcrop in any condition is hard to find as most of the area is covered by regolith and exposed fresh outcrop tends to be at the top of slopes and at the coastline. When drilling on the eastern side of the fault, the top of the slope is also the most likely spot to be hit by lightning as it is also at the

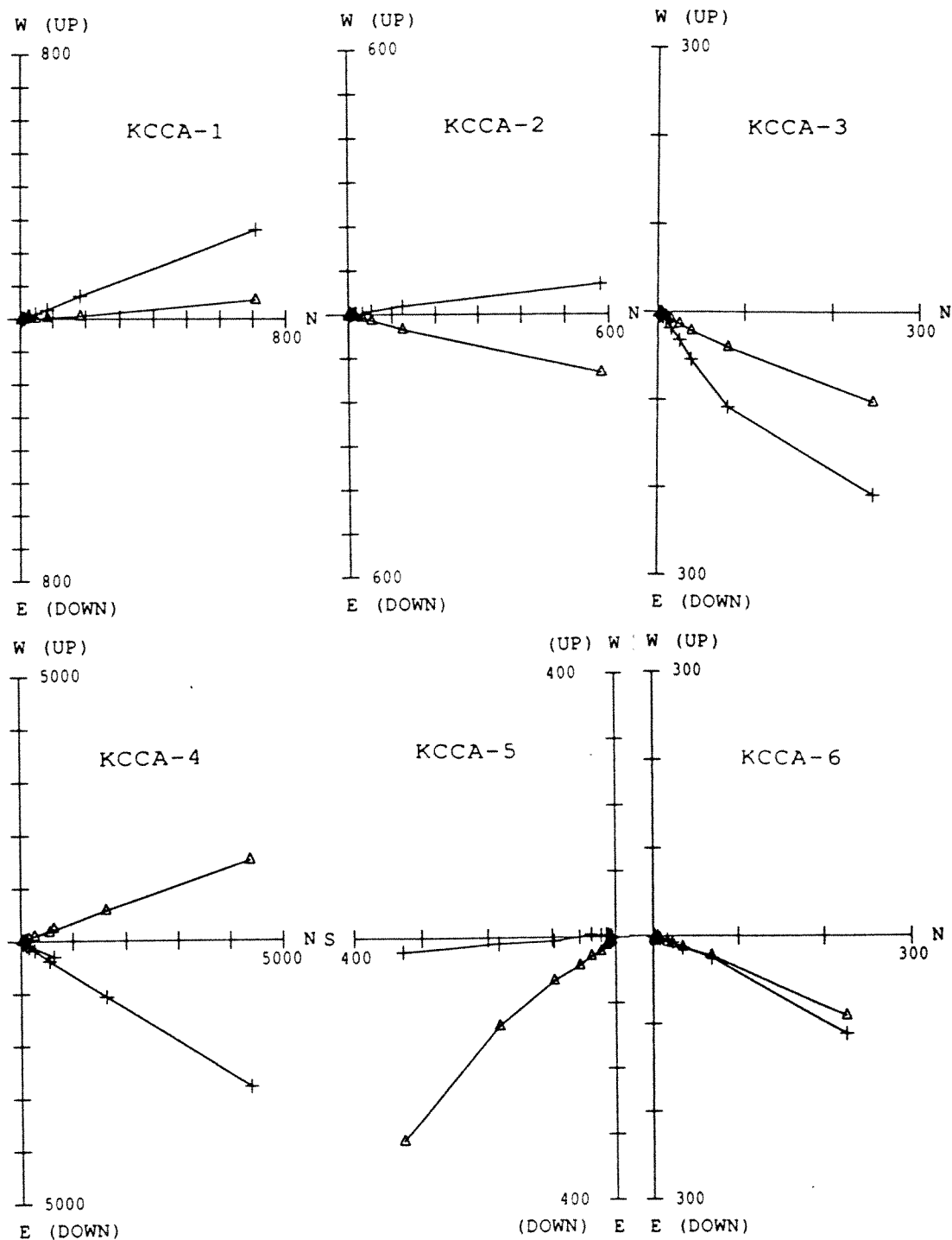


Figure 20. Zijderveld plots of the six samples from site KCCA showing the wide range of magnetic directions characteristic of lightning strikes

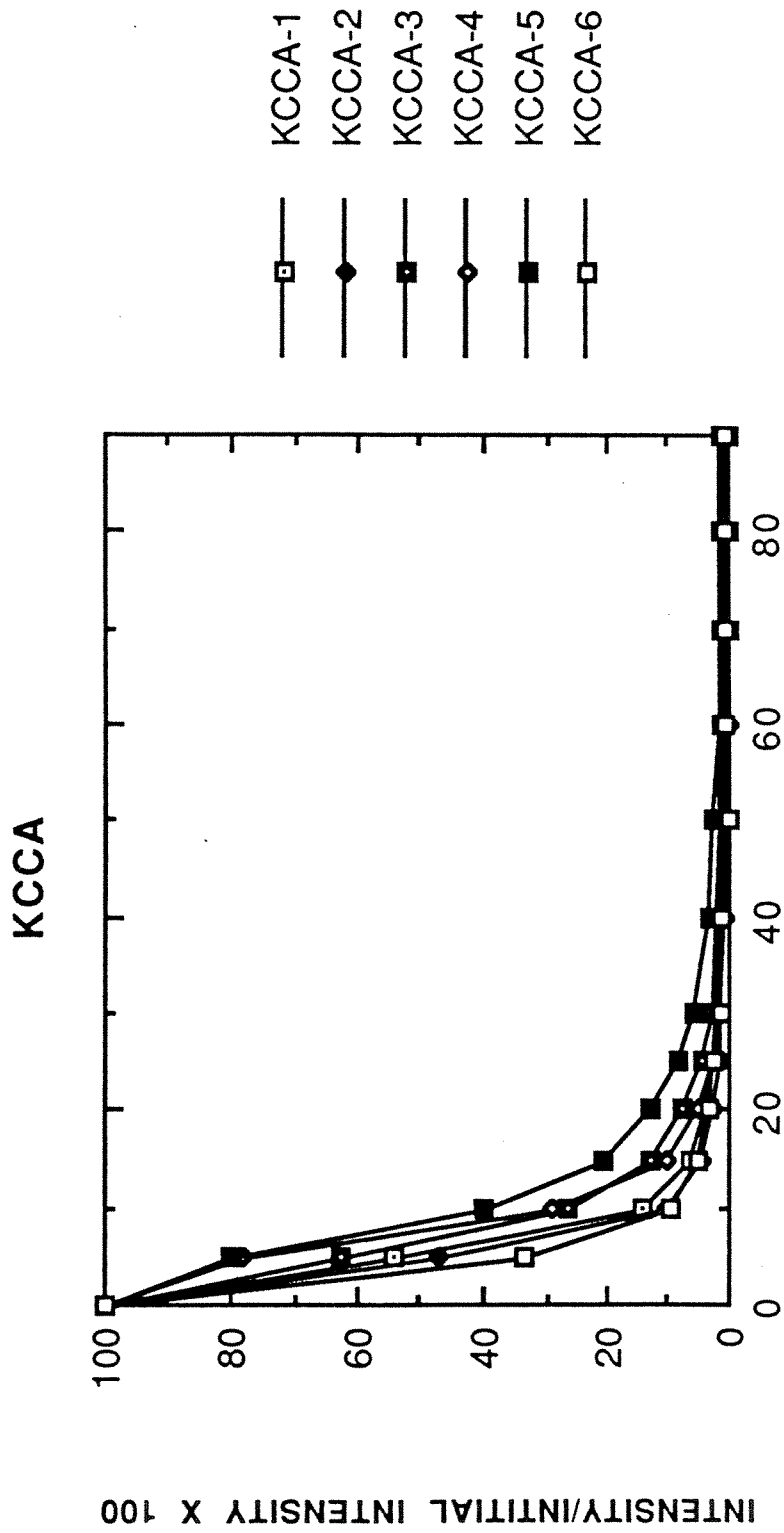


Figure 21. J/J_0 plots of the samples from site KCCA demonstrating the low coercivity of the magnetization typical of a lightning strike.

highest elevation. Drill sites that were not at the top of the slope were chosen in the second summer, but because of the poor exposure of fresh outcrop they had to be on the slopes and not in the valleys. Also different portions of the same pluton were sampled in order to try and avoid the problem. Unfortunately the plan was not successful though as a result, there are some very interest plots of numerous samples exposed to lightning.

VISCOUS SAMPLES

Two sampling sites, JCBA and KQPA, failed to provide any useful magnetic components in the final analysis. The twelve samples of JCBA ranged in initial intensity from 33.12 to 0.66 mT. As can be seen from the representative sampling of J/J_0 and Zijderveld plots of JCBA (fig. 22), intensity increase and decrease and declination and inclination are extremely erratic. Cores were taken from this pluton both summers, but in spite of persistence, all samples are too viscous to consider further. The eleven samples taken from site KQPA had a wide range in intensity, from 20.11 to 0.062 mT. There were samples within the site that had the normal and/or reversed component(s) (fig. 23a. and b.), but there were not enough samples that exhibited this behavior. Many of the samples only yielded viscous results (fig. 23c.) so the site was not statistically sound and was not included in the final analysis.

UNREADABLE LABELS

No usable results were obtained from site KFPA. Only

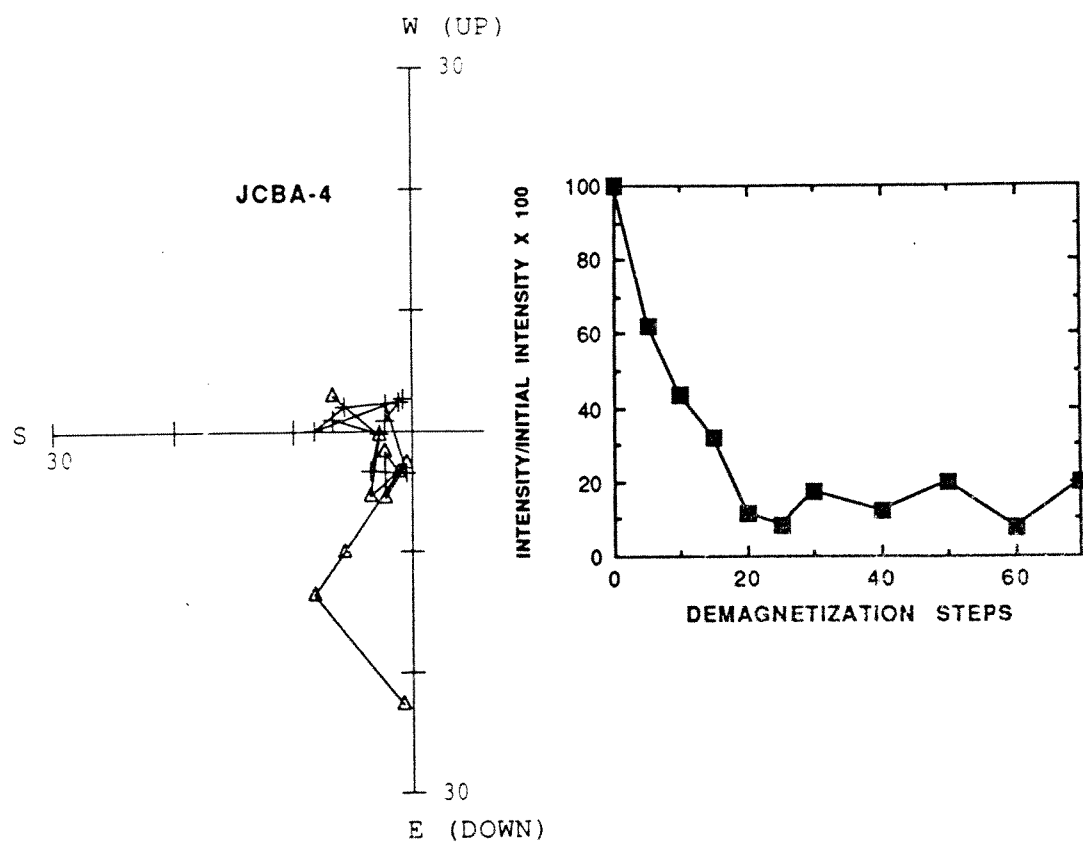


Figure 22. Representative Zijderveld and J/J_0 plots from site JCBA

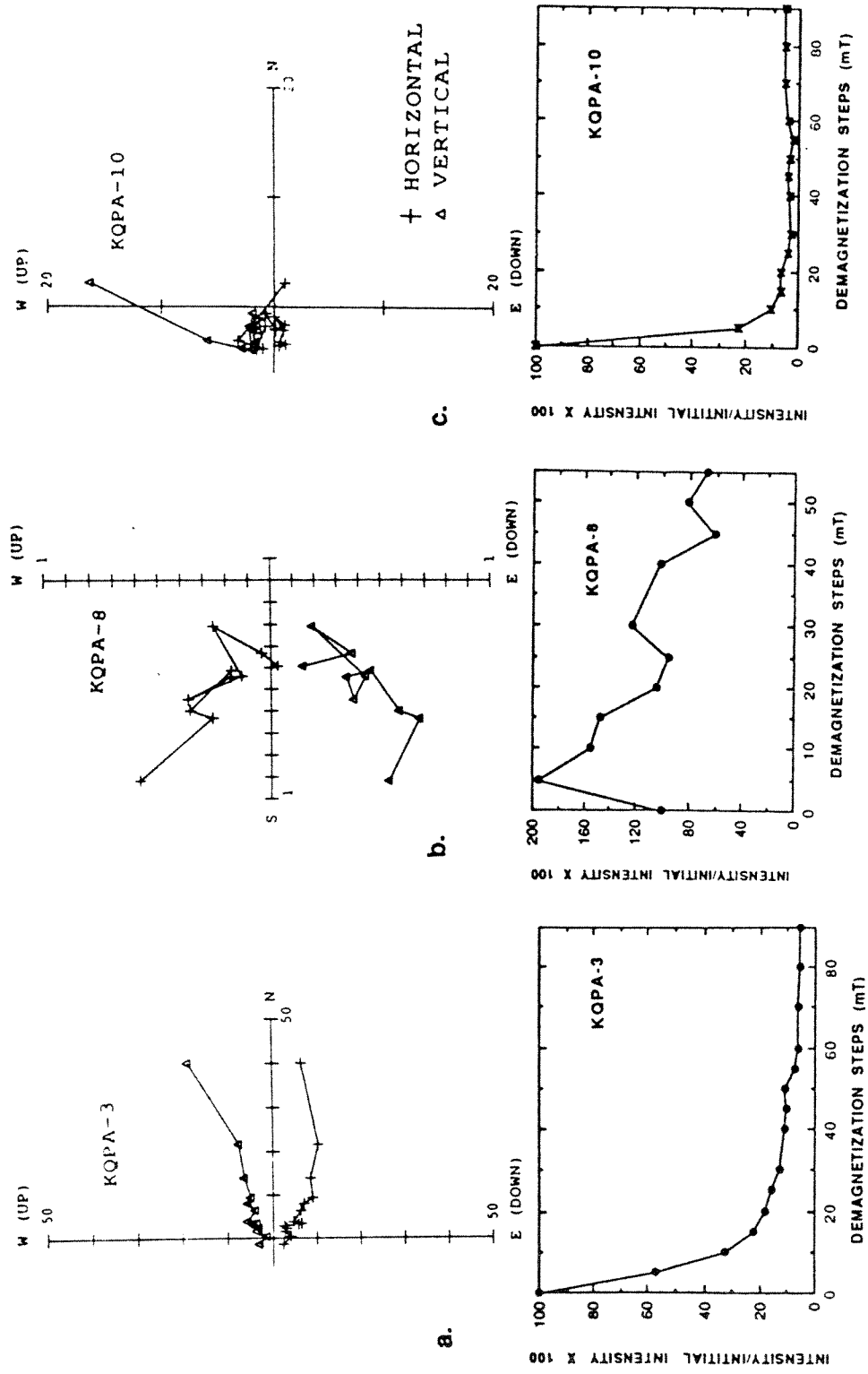


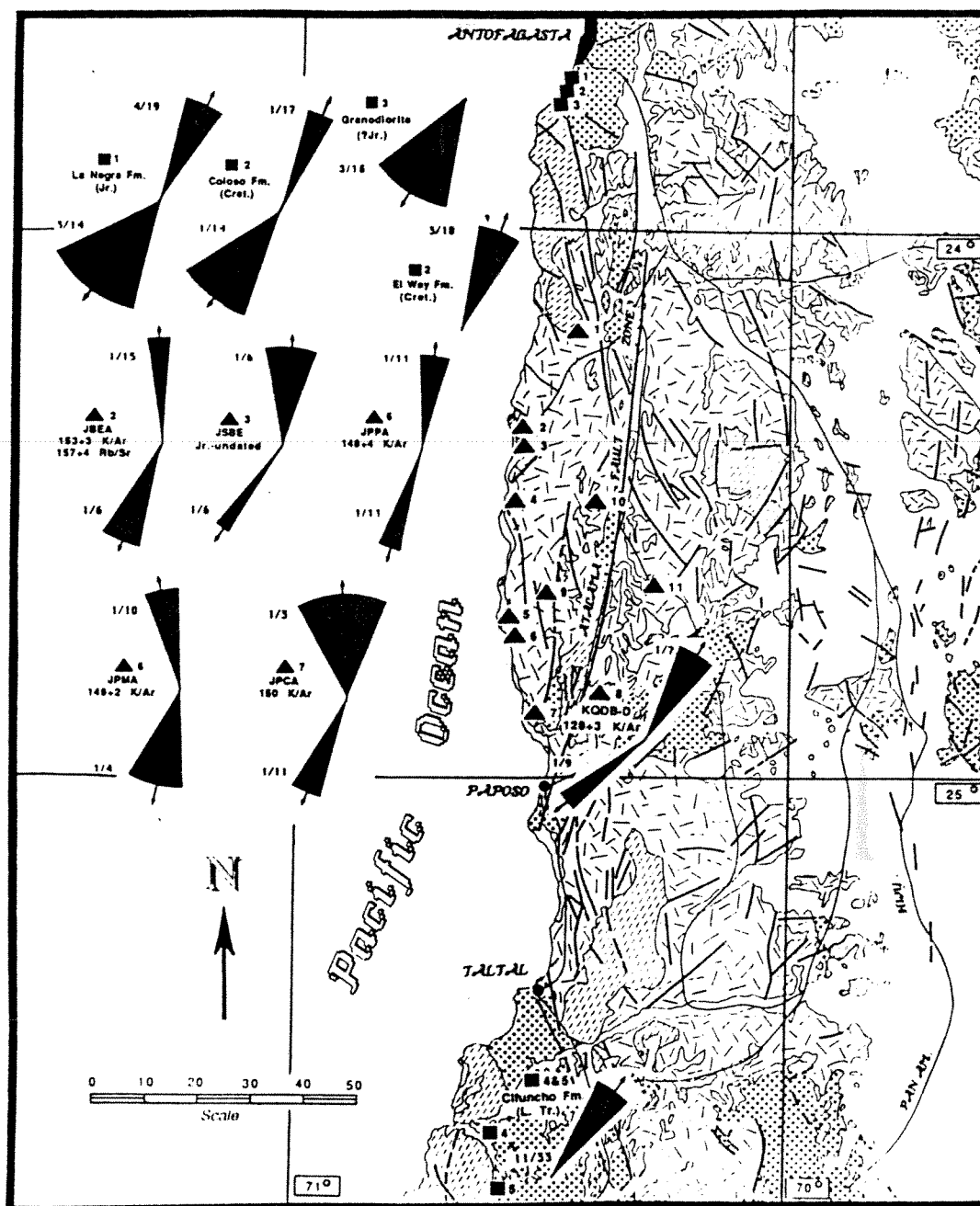
Figure 23. Samples from site KQPA a. with the group's characteristic normal direction, b. with the group's characteristic reversed direction, and c. demonstrating the typical viscous behavior found at this site.

four samples were drilled from here in 1985, and they lost their labels either in transit or while being cut into cores in the laboratory. The labeling problems could not be resolved with any confidence, and the site could not be relocated for resampling in the summer of 1988 so this site had to be disregarded.

DISCUSSION

SUMMARY OF RESULTS

Six of the Jurassic to Cretaceous coastal plutons sampled for this paleomagnetic study yielded statistically significant results at the site level (see Table 1). All six sites had two characteristic directions that were isolated and defined through AF demagnetization, a northerly and up direction and a southerly and down direction (fig. 24). The six normal directions were averaged to produce a regional mean with a declination of 3.4° , an inclination of -38.5° , a k value of 29.5, and an α_{95} of 10.5° . The regional reversed mean direction had a declination of 207.8° , an inclination of 33.8° , a k value of 28.0, and an α_{95} of 10.8° . These two mean directions were then used to calculate paleopoles. The paleopoles calculated from the normal and reversed results have the positions of latitude= 85.8°N , longitude= 338.2°E and latitude= 63.5°S , longitude= 191.9°E respectively. When the two poles are projected on the same hemisphere of a polar projection map, they are seen not to be antipodal (fig. 25). The reversed pole direction is displaced clockwise from the normal pole position. Also, as previously discussed (fig. 8 and 9), the reversed component has a higher coercivity spectrum. While it is not possible to argue that the reversed direction was strictly speaking "a primary" component because the actual time of acquisition has not been better constrained through a fold, conglomerate, or



baked contact test, these two observations offer compelling evidence that the two components represent distinctly different times during the history of the coastal plutonic complexes. The northerly and up direction is softer and closer to the present day field direction. It is interpreted here to reflect a more recent acquisition. The southerly and down direction, which is hard and discordant with respect to the present day field, is interpreted as an older, probably in part primary, component.

In the discussion to follow, this study's results will be compared to three other sets of data. It will be compared to an apparent polar wander path (APW) for South America, with other regional coastal data, and with data from the Andes of Peru to Southern Chile. After these comparisons are made, the tectonic history of the area will be discussed with an emphasis on some of the current models of strike-slip faults and fore arc tectonics.

THE APW FOR SOUTH AMERICA

The APW for South America, as provided by Irving and Irving (1982), was constructed by averaging individual pole determinations from 310 Ma to the present in 30 m.y. windows to determine mean paleopoles every 10 m.y.. This study's results are shown along with the above APW in figure 26. From the Jurassic until the present, the calculated mean paleopoles are not dramatically different from the present dipole field. Therefore, the observed difference in declination between the normal and the reversed poles can not

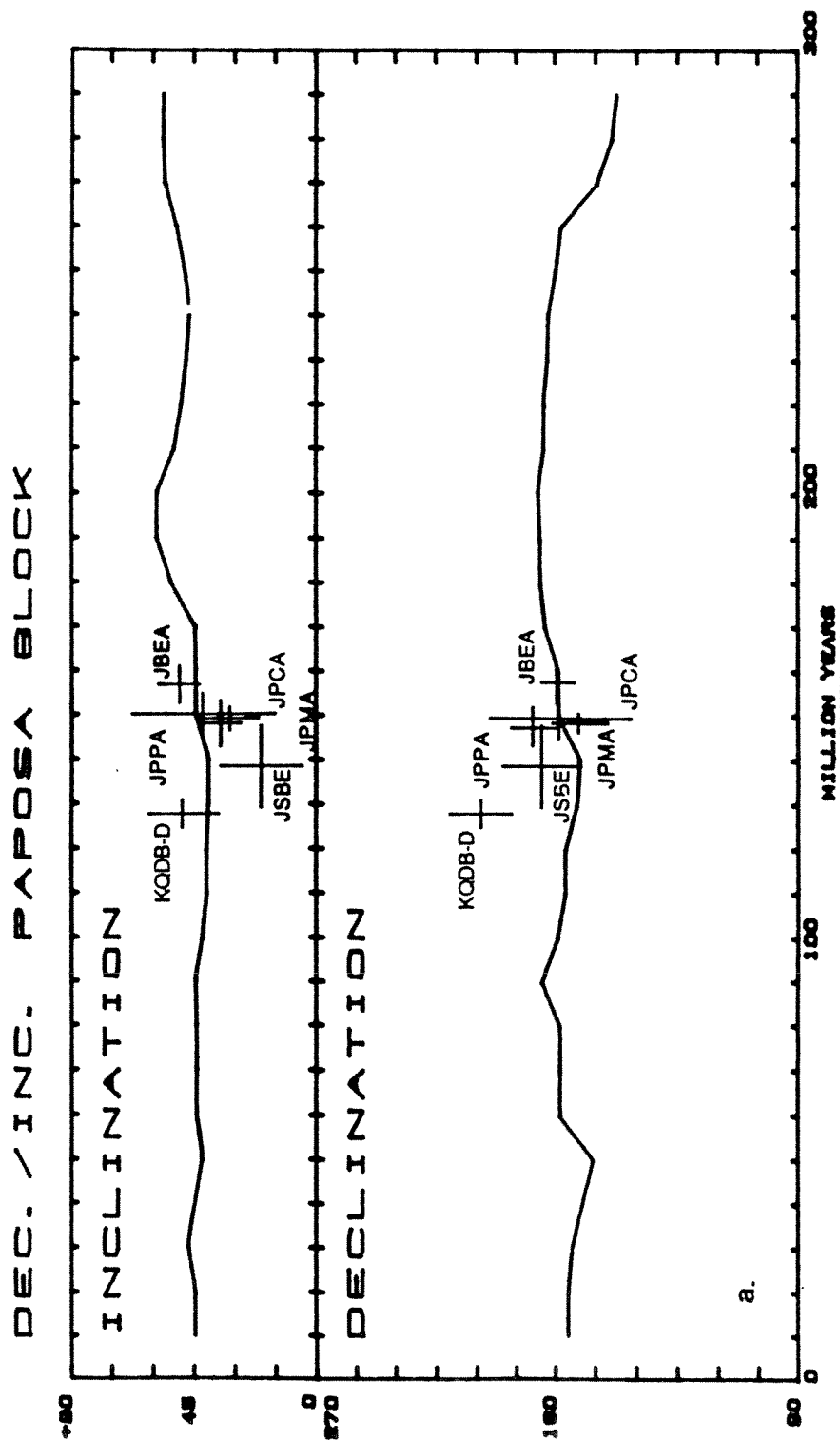
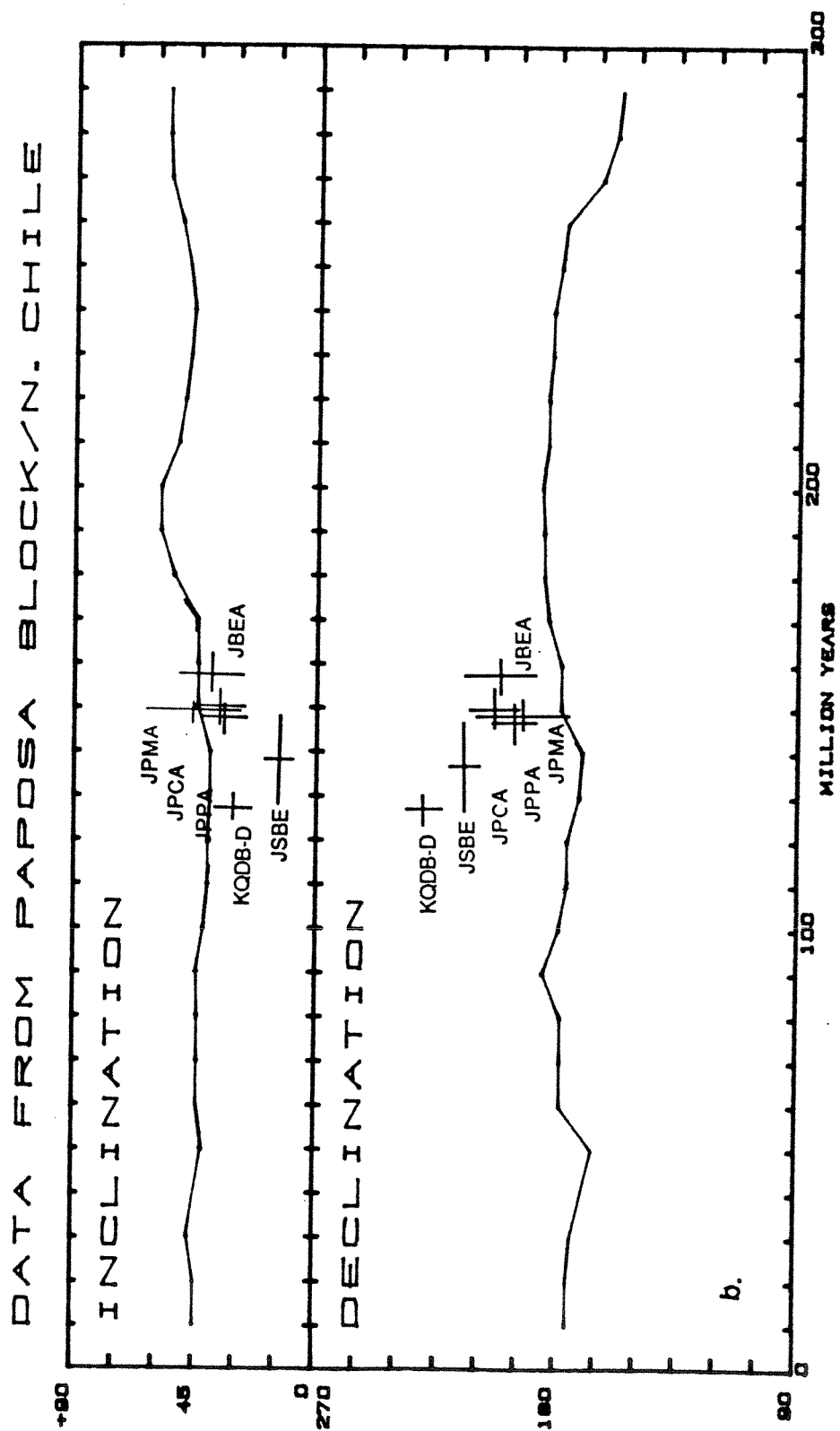


Figure 26. The curve represents the predicted declination and inclination values calculated from the averaged APW path of Irving and Irving, 1982, for South America from 290 to 10 m.y. B.P. The crosses represent the calculated mean declination and inclination for each of the six plutonic sites. a. normal direction, b. reversed direction.



be easily explained by a simple variation in time of acquisition. Secular variation can also be ruled out because the six plutons were sampled over a seventy mile range, and they represent a 29 m.y. age span.

Model site directions, calculated using the running means of Irving and Irving (1982), of rocks located between 24 and 25°S in the age range of 157 to 128 Ma have declinations near 0° (180° for reversed polarity) and inclinations of between approximately 40° and 45°. Plotted along with these model directions are the observed directions for the normal and reversed site means (fig. 27). The calculated mean normal direction of this study is more or less concordant with the expected direction within the limits of confidence, but the calculated reversed mean direction from this study has a slightly discordant inclination of ~6° and a measurable discordant declination of 28°. The inclination is within the error limits, but could also be the result of an unresolved tilt correction since some gentle folding and tilting has been noted regionally (Ferraris and DiBiase, 1978). The observed discordance in declination is well beyond confidence limits and is compatible with significant clockwise rotation.

OTHER REGIONAL RESULTS

There have been three other studies very near the present investigation (see Table 2) that also show evidence for clockwise rotation. The results of Turner et al. (1984) and Hartley et al. (1988) are just to the north and the

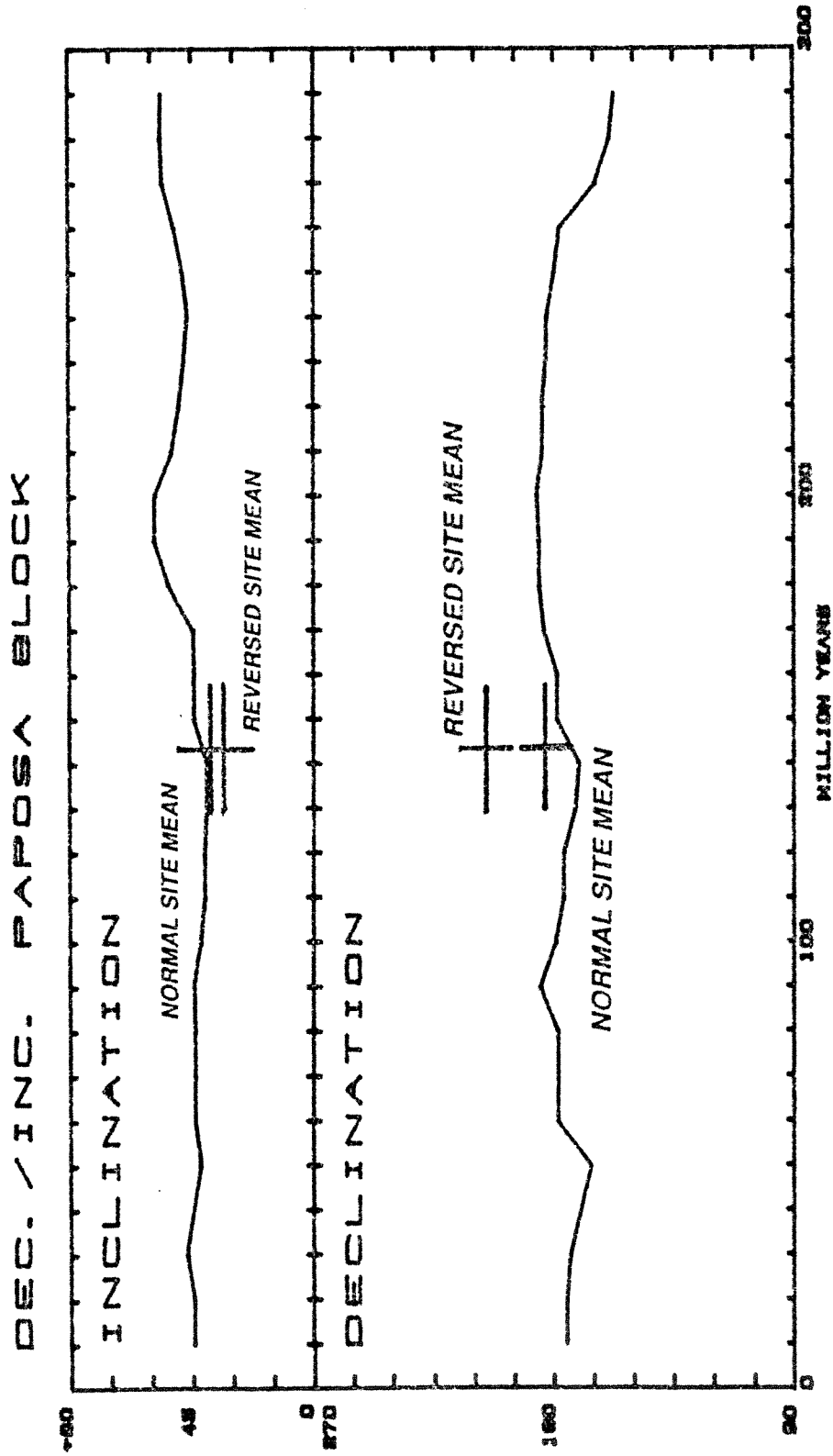


Figure 27. Predicted versus observed declinations and inclinations for the calculated mean declination and inclination for the six sites as a group.

Table 2.

REFERENCE	UNIT	AGE	LONGITUDE	LATITUDE	PALaeOLITE	MEAN DEC. INC	K	alpha_9 dp dm	n SAMPLES
1 Palmer et al., 1980	Camiraca Fm.	157/4 Ma	70.3W	10.6S	012.9E/70.7S	339.6/-35.7	17.9	6.1	4.3/ 7.1
2 Palmer et al., 1980	Arqueros Fm.	Cretaceous	70.9W	29.8S	161W/00.5S	000/-41.5	40		8.4/13.2
3 same as above	Quebrada Marquesa Fm.	Cretaceous	70.9W	29.9S	161.1W/77S	014.5/-46	63		4.9/ 7.5
4 same as above	Vialta Fm.	Cretaceous	70.8W	29.8S	111W/92S	006.5/-55.5	54		6.0/ 8.1
5 same as above	Elquiños Fm.	Cretaceous	70.8W	29.8S	076E/83S	356.0/-41.5	26		10.7/16.5
6 same as above	ave. site pole-except Elquiños Fm.	Cretaceous	71W	25S	209E/81S			4.5	30 sites
7 Turner et al., 1984	Coloso Fm.	Early Cretaceous	70.4W	23.8S	192E/70S	021/-36	20.3	6.8	17 sites
8 same as above	Coloso Fm.	Early Cretaceous	70.4W	23.8S	195E/55S	217 /31	7.6	20.0	9 sites
9 Beki et al., 1981	coastal volcanic rocks	late Middle Albian	75-00W	5-15S	000.5E/58S			5.1	12 sites
10 same as above	Chalec Fm.	Albian	70.3W	7.1S	001.6E/52.0S	321.7/-22.6	36	10.2	4.7/ 8.8
11 same as above	Parlatambo Fm.	Albian	70.3W	7.1S	003.4E/38.1S	307.5/-21.1	134	5.4	3.1/ 5.8
12 same as above	Tunagual Fm.	Cenomanian	70.2W	5.9S	339.7E/66.7S	339.4/-32.2	103	5.1	3.2/ 5.7
13 Beki et al., 1985	Atajana Fm.	Lower Cretaceous	70.3W	10.6S	037.9E/74.7S	345.1/-25.6	46	4.1	2.4/ 4.4
14 same as above	Arica dike swarm	post Lower Cretaceous	70.3W	10.6S	352.4E/77.2S			3.3	19 sites
15 Hay & Butler, 1985	Puente Piedra Fm.	90/5 Ma	77.1W	11.9S	359.3E/73.3S	343.2/-28.6	167.4	3.4	3.7/2.0
16 Beck et al., 1986	San Fernando ash-flow tuff	approx. 100 Ma	71W	34S	191.6E/75.5S	016.9/-50.2	27.7	6.0	22 sites
17 same as above	Chacabuco ash-flow tuffs	approx. 65 Ma	71W	33S	330.3E/77.5S	340.9/-60.9	22.3	8.3	15 sites
18 Forsythe et al., 1987	Pastos Blancos Fm.	Late Carb.-Early Permian	70.1W	31.1S	200.3E/68.7S	33.1/-44.4	65	6.9	5.5/ 8.7
19 same as above	Cifuncho Fm.	Late Triassic	70.6W	25.6S	217.1E/57.5S	036.6/-50.0	24	9.6	8.6/12.8
20 same as above	Pichidangui Fm.	Late Triassic	71.5W	31.2S	070.7E/44.1S	353.1/-50.0	69	5.8	5.2/ 7.8
21 same as above	Pichidangui Fm.	Late Triassic	71.5W	31.2S	277.5E/59.0S	191.7/674.6	134	6.6	10.9/12
22 Jesinkey et al., 1987	La Tabla Fm.	Upper Carb.-Permian	69.3W	24.5S	347E/51S	136.9/458.8	72.4	5.7	10 sites
23 same as above	combined Pular & Cas Fm.s	U.Carb.-Permian (290+7Ma)	69W	24S	350E/57S	143.0/456.1	26.3	8.6	10 sites
24 Irwin et al., 1987	dikes & plutons	approx. 170 Ma	71.7W	37-33.5S	036.7E/45.9S	002 /-49.2	17.4	11.9	8 sites
25 same as above	dikes and plutons	approx. 145 Ma	71.7W	37-33.5S	207.4E/40.3S	011.4/-54.3	21.6	9.5	10 sites
26 Bartley et al., 1988	Jurassic granodiorites	159-134 Ma	70W	24S	189E/59S	212/428	36.0	20.8	3 sites
27 same as above	La Negra Fm.	Middle Jurassic	70W	24S	190E/66S	025/-33	70.8	11.0	4 sites
28 same as above	La Negra Fm.	Middle Jurassic	70W	24S	220E/57S	217/450	17.2	26.4	3 sites
29 same as above	El Way Fm.	131-124 Ma	70W	24S	144E/70S	020/-32	117.1	11.4	3 sites

results of Forsythe et al. (1987) are just to the south. The declination and the cones of confidence of those calculated poles are shown in figure 24. When all the measured results from the area are compared to the expected results of Irving and Irving (1982), they show there is no notable discrepancy in mean inclination and the declinations show discordance that would be compatible with clockwise rotation of 20 to 30° (fig. 28). Unlike the present study, the results from Hartley et al. (1988) have undergone tilt corrections for bedding orientations of 120/20SW for the Jurassic granodiorites and the La Negra Fm. and 105/20SW for the Cretaceous El Way Fm. With these corrections, they similarly indicate a significant clockwise rotation of ~25°. The results of Forsythe et al. (1987) were from Triassic volcanics. Here, the normal component failed a fold test and the insitu directions suggested approximately 20°(+) of clockwise rotation. One of the differences between the present study and previous ones is found in comparing the normal direction poles. The normal pole calculated from the present data is concordant with the present day field while previously calculated normal poles seem to have also been affected by clockwise rotation. However, previous results have not attempted to isolate hard and soft components to the same degree, and it could be that the other normal components are composed of mixed early (hard) and late (soft) contributions.

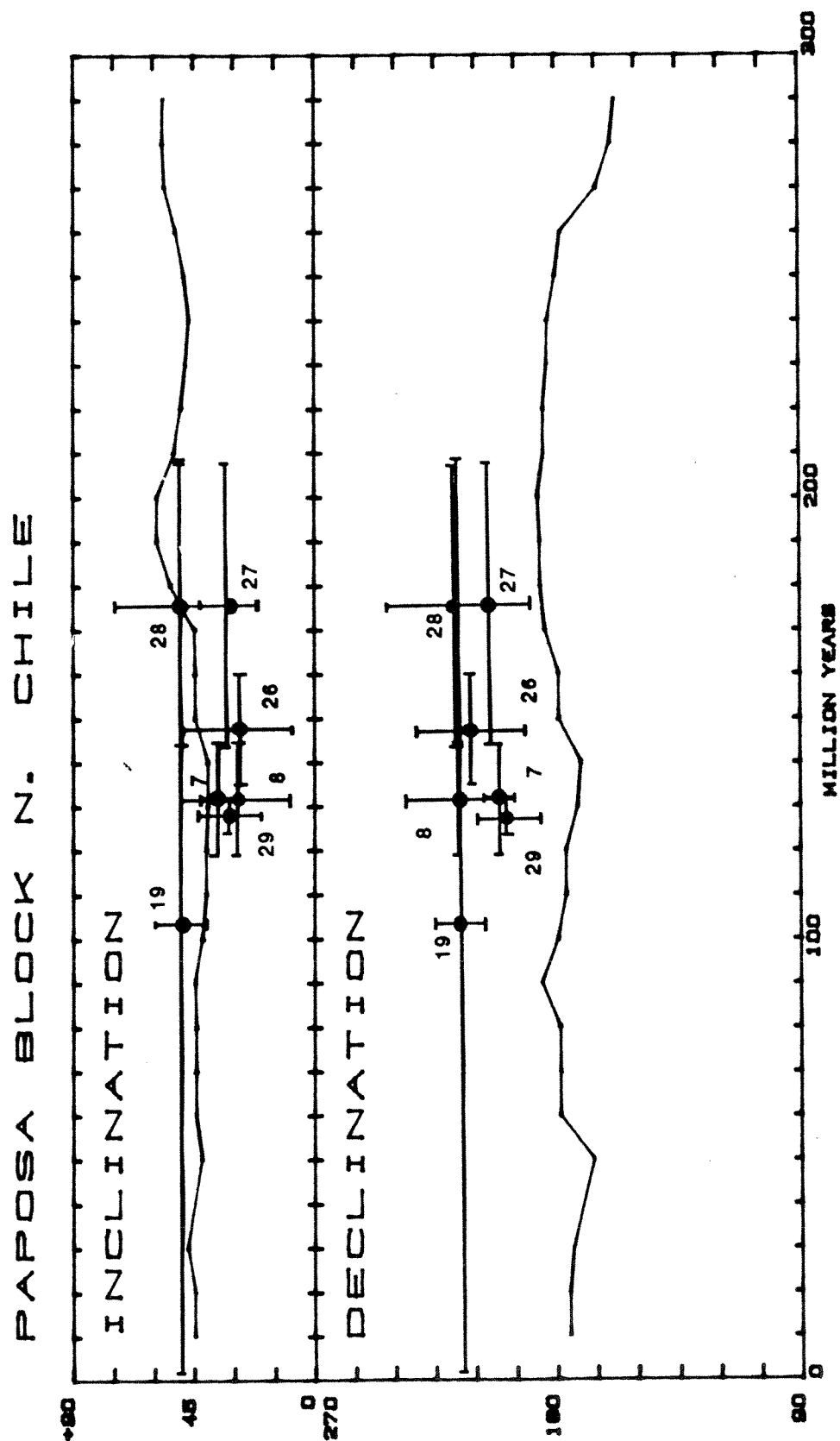


Figure 28. Predicted versus observed declinations and inclinations for the calculated means from the regional data.

ANDEAN PALEOMAGNETIC DATA

On a broader scale, the results from the Jurassic to Cretaceous plutons can be compared to the growing body of paleomagnetic data from the Andes of Peru to Central Chile (Table #2 and fig. 29). The results from the region north of 19°S (Northern Chile into Peru) generally exhibit counterclockwise discordance with respect to cratonic South American APW data (Heki et al, 1983; May and Butler, 1985; and Beck, 1986). In the region south of 19°S, the results have the opposite sense of discordance. While there seems to be a predictable sense of discordance, clockwise or counterclockwise, there is no uniformity in the extent or timing of rotation. In the coastal regions of Chile, for example, the amounts of rotation observed for Jurassic to Early Cretaceous plutonic sites varies from one coastal block to another from approximately 0° to 30°. There is also no simple apparent correlation of the amount of rotation with age. Miocene intrusions along the Liquini-Ofqui fault zone have been found with rotations comparable to that of some of the more discordant Jurassic ones.

The results from two paleomagnetic studies, with sampling sites in the Main Cordillera, show either no rotation or small amounts of rotation. Jesinkey et al. (1988) investigated formations that were Late Paleozoic in age from lat. ~24°S, long. ~69°W (see Table #2). The timing of the acquisition of the magnetism measured was constrained by positive conglomerate tests and by tilt (bedding)

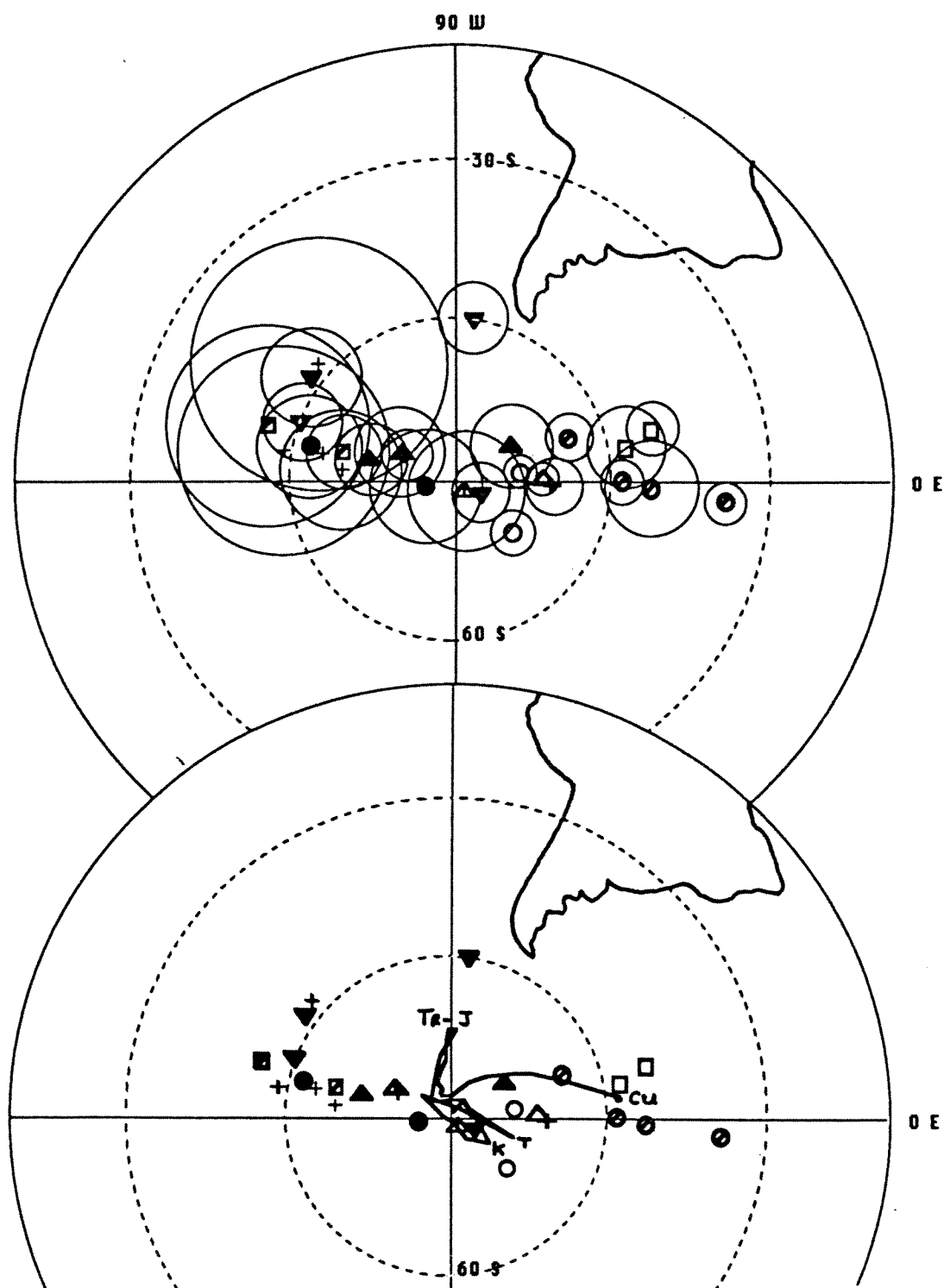


Figure 29. Polar projection map showing the published paleomagnetic poles listed in Table #2. Also shown, is the polar wander path from 290 to 0 m.y. B.P. as calc by Irving and Irving, 1982.

corrections. A Cretaceous section near La Serena was the subject of a study undertaken by Palmer et al. (1980) (see Table #2). They found the calculated paleomagnetic poles from the section were basically concordant with the mid to late Cretaceous poles derived from rock units of the stable craton of South America. The age of the magnetization component was confirmed to be pre-Tertiary in age by a positive fold test. Though more data is needed, it appears that the rotations are restricted to the Coastal Cordillera in northern Chile.

In summary, paleomagnetic investigations of Jurassic to Cretaceous intrusive and extrusive rocks as well as the coeval sedimentary strata from the northern coastal province situated adjacent to the Atacama Fault zone indicate about the same amount of clockwise rotation of $\sim 24-32^\circ$. The present study from this area also presents evidence of a secondary magnetic component that shows no rotation with respect to the cratonic South American APW.

In comparison to these discordant Jurassic and Cretaceous results, Garcia et al. (1988) has documented similar degrees of clockwise rotation in much younger units (as young as 3 to 5 Ma) situated along the Liquine-Ofqui fault zone to the south (see fig. 7). The Liquine-Ofqui fault zone is thought to be an active dextral strike-slip fault within the south volcanic field of Chile (Forsythe and Nelson, 1985). The formations and plutons of the northern coastal province on the other hand are situated along the

Atacama Fault Zone where the strike-slip activity may have occurred at an earlier stage (100(+)Ma). Similarly the magmatic activity in this zone died in the Cretaceous.

MODELS

Oroclinal bending: It has been suggested by Heki et al. (1983) that the systematic counterclockwise to clockwise discordance from Peru to Chile in observed paleomagnetic declinations in coastal units of Jurassic to Tertiary ages could be explained by a simple process of oroclinal bending following some of the initial ideas of Carey, 1955.

Unfortunately, the simple oroclinal bending model can not explain two observations. First, it can not easily account for the variation in amounts of discordance (from 0° to 30°) that have been measured in rocks of the Coastal Cordillera. It is also not possible for this hypothesis to explain the unrotated results that have been documented in the Main Cordillera (Jesinkey et al, 1987; Palmer et al, 1980).

Oblique Subduction Models

Presently, the dominant model used to explain the rotations of the Coastal Cordillera is one in which oblique subduction plays the dominant role. Oblique subduction has been hypothesized to be the driving force behind the major strike-slip faults (associated with subduction zones) that are not only in Chile (Herve, 1976; Beck, 1988), but also around the world (Fitch, 1972; Beck, 1983; Jarrard, 1986). In the model's simplest form, oblique subduction drives regional shear along a subvertical fault plane parallel to

the subduction zone. The motion in the zone of shear in turn causes the insitu rotation of small coastal blocks. The amount of local block rotation is proportional to the amount of shear across the zone, and the latter is in turn proportional to the amount of oblique subduction. The simpler kinematic arguments have been laid out in the paper by Jarrard (1986). The discussions of Fitch (1972), as well as Beck (1983), however, acknowledge that other factors may also be important. Specifically, factors that may control the internal strength of the overriding plate, such as the presence or absence of magmatism, or factors influencing the coupling forces acting across the plate boundary such as the angle of subduction, are also acknowledged to be relevant. Despite acknowledgement of these factors, no quantitative or even semi-quantitative kinematic/mechanical model has been proposed.

In South America, the amount and the timing of rotation do not show good correlation with oblique plate motion. As discussed above, the results from the area surrounding the younger Liquine-Ofqui Fault Zone show similar amounts of rotation to the results surrounding the older Atacama Fault System. The inconsistent pattern of faulting and rotations in space and time would require a very complex pattern of relative plate motions within a simple kinematic model for oblique plate motion. It seems something else, a 'trigger' mechanism is needed to make the forearc sensitive to oblique subduction.

An 'Indenter' analog

Forsythe and Nelson (1985) presented an indenter model to explain the dextral strike-slip motion along the Liquini-Ofqui Fault (LOF). The spreading ridges at the triple junction of the Nazca, Antarctic, and South American plates were being subducted near the focal point of the LOF zone in the Late Tertiary. In their model, these spreading ridges act as stress indenters to the continental margin. The increase in topography and heat flow as the left laterally offset spreading ridges are subducted would create the highest stress at the triple junction. The stress would decrease laterally away from this point. Since the plate convergence vector was nearly parallel to the fracture zones, this stress configuration would be long lived. This is postulated to have weakened the margin sufficiently to have initiated or continued slip on the LOF.

The data from Peru to Chile have far to simple a regional pattern to their senses of discordance to be easily explained by an indenter model. Colliding features such as seamounts, aseismic or active ridges, generally are limited in regional extent, and are highly unstable in their locations. Just as it would be unlikely that the disorder in the patterns of rotations could be explained by a simple oblique subduction model, it would equally be unlikely that the order, e.g. regionally counterclockwise in Peru, and clockwise in Chile, could be explained away by some systematic series of 'collisional' or indentation events.

This does not discount the importance of either model, but individually they can not easily account for the complex tectonic history of the coastal Andes of Peru and Chile.

Summary of models

In summary, in addition to the oblique subduction, it appears we must look for other factors. In the background presence of some component of oblique subduction, we can conceptually refer to the other factor as a 'trigger'. This factor sensitizes the margin in some unknown fashion to the oblique component and initiates a strike-slip and block rotational event. In this way, the temporally punctuated and regionally variable geologic record of block rotation and faulting is one of not just oblique subduction, but more precisely the 'triggering processes'.

What are the processes as they pertain to the rotations observed in the coastal plutons of northern Chile? They can be viewed as either strength or stress related. Strength is an internal property of the lithosphere. Changes in strength will affect how a body responds to stress. Strength, for example, will likely change with an increase in regional heat flow. Stress is largely an external condition that is applied to a body. Changes in the environment create changes in the stress. A change in stress would result from changes in the subduction angle or the rates and directions of relative plate motion.

There is very little known about the specific relative plate motions in northern Chile during the Jurassic to the

Cretaceous so it is not possible to argue in a rigorous way about changes in the stresses that may have operated in the area. The geologic record of the study area during this period, however, clearly documents the eastward migration of the axis of magmatism through time. As figure six illustrates, by the Late Cretaceous to Early Tertiary magmatism had migrated eastward, away from the Atacama Fault Zone. Given what we presently understand, it seems most logical to argue that this migration ended a phase of sensitivity and deformation related to oblique subduction. In other words, an arc region, previously located along the Coastal Ranges, had thermally weakened the region, 'triggering' dextral shear and clockwise block rotation along the Atacama Fault Zone in the presence of some background component of oblique subduction.

REFERENCES

- Allen, C.R., Transcurrent faults in continental areas-A symposium on continental drift, Phil. Trans. Roy. Soc. London, 258, 82-89, 1965.
- Arabaz, W.J., Geological and geophysical studies of the Atacama fault zone in northern Chile. Ph.D. Thesis, Inst. Tech., Pasadena, 1-359, 1971.
- Bahlburg, H., C.Breitkreut, and W. Zeil, Paleozoic basement development in northern Chile (21°-27°S), Geol. Rundschau, 72, 633-646, 1987.
- Beck, M.E. Jr., Analysis of Late Jurassic-Recent paleomagnetic data from active plate margins of South America, Jour. of S.Am.Earth Sci., 1, 39-52, 1988.
- Beck, M.E., Jr., R.E. Drake, and R.F. Butler, Paleomagnetism of Cretaceous volcanic rocks from central Chile and implications for the tectonics of the Andes, Geology, 14, 132-136, 1986.
- Beck, M.E., Jr., On the mechanism of tectonic transport in zones of oblique subduction, Tectonophysics, 93, 1-11, 1983.
- Boric, R., F. Diaz, and V. Maksaev, Magmatic events and related metallogenesis in the Antofagasta region, Northern Chile, Comunicaciones, Dept. Geol. Univ. de Chile, Santiago, 35, 37-43, 1985.
- Cande, S., Nazca-South America plate interactions, 80 My to present, EOS. 64-865, 1983.
- Carey, S.W., The orocline concept in geotectonics, Proc. R.Soc. Tasmania, 89, 255-288, 1955.
- Coira, B., J. Davidson, C. Mpodosi, and V. Ramos, Tectonic and magmatic evolution of the Andes of northern Argentina and Chile, Earth Sci. Rev., 18, 303-332, 1982.
- Collinson, D. W., Methods in Rock Magnetism and Paleomagnetism, Chapman and Hall, New York, 503 p., 1983.
- Dalziel, I.W.D., and R.D. Forsythe, Andean evolution and the terrane concept, in: Howell et al., eds., "Tectono-stratigraphic Terranes of the Circum-Pacific regions" American Association of Petroleum Geologists, Circum Pacific Council for Energy and Mineral Resources, Earth Science Series v. 1, Tulsa, OK, p. 565-581. 1984.
- Dunlop, D.J., On the use of Zijderveld vector diagrams in multicomponent paleomagnetic studies, Phys. Earth Planet.

Inter., 20, 12-24, 1979.

- Evans, M.E., and M.W. McElhinny, An investigation of the origin of stable remanence in magnetite-bearing igneous rocks, Jour. Geomag. Geoelect., 21, 757-773, 1969.
- Ferraris, F.B., Geologia de la Cordillera de la Costa, in Carta Geologica Chile, scale 1:250,000, 26, Servicio Nacional de Geologia y Minería, Santiago, 1978.
- Ferraris, F.B., and F.F. DiBiase, Geologia de la Hoja Antofagasta, in Carta Geologica Chile, scale 1:250,000, 30, Servicio Nacional de Geologia y Minería, Santiago, 1978.
- Fisher, R.A., Dispersion on a sphere, Proc. R. Soc. London, Ser. A, 217, 295-305, 1953.
- Fitch, T.J., Plate convergence, transcurrent faults and internal deformation adjacent to Southeast Asia and western Pacific, Journ. Geophys. Res., 77, 4432-4461, 1972.
- Forsythe, R.D., D.V. Kent, C. Mpodosis, and J. Davidson, Paleomagnetism of Permian and Triassic rocks, central Chilean Andes, in: Gondwana Six, D.H. Elliot, J.W. Collinson, and G.D. McKenzie, eds., Am. Geophys. Union, Geophysical Monogr. Ser., 241-252, 1987.
- Forsythe, R., and E. Nelson, Geological manifestation of ridge collision: evidence from the Golfo de Penas-Taitao Basin, Southern Chile, Tectonics, Vol. 4, No. 4, 447-495, 1985.
- Garcia, A.R., M.E. Beck Jr., R.F. Burmester, F. Munizaga, and F. Herve, Paleomagnetic reconnaissance of the region de los Lagos, southern Chile, and its tectonic implications, Revista Geologica de Chile, 15 13-30, 1988.
- Garcia, F., Geologia del Norte Grande de Chile, in: Simposium Sobre el Geosynclinal Andino, Soc. Geol., Chile Publ., vol. 3, 183 pp., Sociedad Geologica de Chile, Santiago, 1967.
- Hartley, A.J., P. Turner, G.D. Williams, and S. Flint, Paleomagnetism of the Cordillera de la Costa, northern Chile: evidence for local forearc rotation, Earth Planet. Sci. Lett., 89, 375-386, 1988.
- Heki, K., Y. Hamono, and M. Kono, Rotation of the Peruvian block from paleomagnetic studies of the central Andes, Nature, 305, 514-516, 1983.
- Heki, K., Y. Hamono, H. Kinoshita, A. Taira, and M. Kono,

- Paleomagnetic study of Cretaceous rocks of Peru, South America: evidence for rotation of the Andes, *Tectonophysics*, 108, 267-281, 1984.
- Heki, K., Y. Hamono, and M. Kono, Paleomagnetic study of the Cretaceous Atajana Formation and the Arica Dike Swarm, Northernmost Chile, *J. Geomag. Geoelectr.*, 37, 107-117, 1985.
- Herve, F., Estudio geologico del la falla Linguine-Reloncavi en el area de Linguine: antecedentes de un movimiento 1976 transcurrente: Santiago, Chile, *Acta I Congreso Geologico Chileno*, vol. 1, B39-B56, 1976.
- Irving, E., and G.A. Irving, Apparent polar wander paths Carboniferous through Cenozoic and the assembly of Gondwana, *Geophys. Surv.*, 5, 141-188, 1982.
- Irwin, J.J., W.D. Sharp, R.R. Spangler, and R.E. Drake, Some paleomagnetic constraints of the tectonic evolution of the Coastal Cordillera of central Chile, *J. Geophys. Res.*, 92, 3603-3614, 1987.
- Jarrard, R.D., Terrane motion by strike-slip faulting of forearc slivers, *Geology*, 14, 780-783, 1986.
- Jesinkey, C, R.D. Forsythe, C. Mpodosi, and J. Davidson, Concordant Late Paleozoic paleomagnetizations from the Atacama Desert: implications for tectonic models of the Chilean Andes, *Earth Planet Sci. Lett.* 85, 461-472, 1987.
- Kirschvink, J.L., The least-squares line and plane and the analysis of paleomagnetic data, *Geophys. J. R. Astron. Soc.*, 62, 699-718, 1980.
- Maksaev, V., Mesozoico a Paleogeno de la region de Antofagasta, in: *Seminario Actualizacion de la Geologia de Chile*, Serv. Nac. de Geol. y Min. Santiago, C1-C20, 1984.
- May, S.R., and R.F. Butler, Paleomagnetism of the Puente Piedra Formation, Central Peru, *Earth Planet. Sci. Lett.*, 72, 205-218, 1985.
- McElhinney, M.W., *Paleomagnetism and plate tectonics*, Cambridge University Press, 358 p., 1973.
- Mortimer, C., Drainage evolution in the Atacama desert of Northern Chile, *Revista Geol. Chile*, 11, 3-28, 1980.
- Mortimer, C., and N.S. Rendic, Cenozoic studies in northernmost Chile, *Geol. Rundsch.*, 64, 395-420, 1975.
- Mpodosi, C., and V. Ramos, The Andes of Chile and

Argentina, in preparation.

Naranjo, J.A., F. Herve, X. Prieto, and F. Munizaga, Actividad Cretacica de la Falla Atacama al este de Chanaral: milonitizacion y plutonismo, Comunicaciones, Dept. de Geol., Univ de Chile, Santiago, 34, 57-66, 1984.

Palmer, H.C., A. Hayatsu, and W.D. McDonald, The middle Jurassic Camaraca Formation, Arica, Chile: paleomagnetism, K-Ar age dating, and tectonic implications, Geophys. J. R. Astron. Soc., 62, 155-172, 1980a.

Palmer, H.C., A. Hayatsu, and W.D. McDonald, Paleomagnetic and K-Ar age studies of a 6 km-thick Cretaceous section from the Chilean Andes, Geophys. J. R. Astron. Soc., 62, 133-153, 1980b.

St.Armand, P., and C.R. Allen, Strike-slip faulting in northern Chile (Abs), Geol.Soc.Am.Bull., 71, 1965, 1960.

Servicio Nacional de Geologia y Minería, Mapa Geologico de Chile, scale 1:1,000,000, Escobar, F.T., ed. , no. 1 & 2, Santiago, Chile, 1982.

Thiele, R., M. Pinchiera, Las megafallas los Colorados-Portezuelo tatará y la Sosita-Huanteme, en la extension sur de la zona de falla Atacama, al noroeste de Vallenar, Comunicaciones, Dept. de Geol., Univ de Chile, Santiago, 34, 67-70, 1984.

Turner, P., H. Clemmey, and S. Flint, Paleomagnetic studies of a Cretaceous molasse sequence in the central Andes (Coloso Formation, Northern Chile), J. Geol. Soc. London, 141, 869-876, 1984.

Zijerveld, J.D.A., A.C. demagnetization of rocks: analysis of results, in: Methods in Paleomagnetism, eds. D.W. Collinson, K.M. Creer, and S.K. Runcorn, Elsevier Scientific Pub. Co., New York, p. 245-286, 1967.